

# Directed Palladium-Catalyzed $\gamma$ -C(sp<sup>3</sup>)-H Alkenylation of (Aza and Oxa) Cyclohexanamines with Bromoalkenes: Bromide Precipitation as an Alternative to Silver Scavenging

Karthik Gadde,<sup>£</sup> Narendraprasad Reddy Bhemireddy,<sup>£</sup> Juliane Heitkämper,<sup>£</sup> Ainara Nova,<sup>\*</sup> and Bert U. W. Maes<sup>\*</sup>



Cite This: *ACS Catal.* 2024, 14, 1157–1172



Read Online

ACCESS |

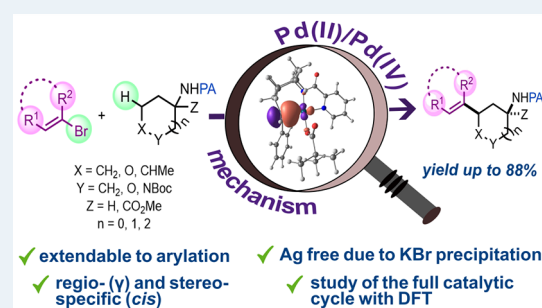
Metrics & More

Article Recommendations

Supporting Information

**ABSTRACT:** Directed palladium-catalyzed coupling of remote C(sp<sup>3</sup>)-H bonds of aliphatic amines with organohalides is a powerful synthetic tool. However, these reactions still possess limitations with respect to cost and resource efficiency, requiring more reactive iodinated reactants and superstoichiometric silver salt reagents. In this work, an efficient regio- and stereospecific silver-free Pd-catalyzed  $\gamma$ -C(sp<sup>3</sup>)-H alkenylation of cyclohexanamines and heterocyclic analogues with bromoalkenes is reported, which can also be applied on five- and seven-membered rings. DFT methods revealed that the oxidative addition of the organobromide to Pd(II) is not the rate-limiting step but rather  $\gamma$ -C(sp<sup>3</sup>)-H bond activation in the substrate. The lowest energy complex in the catalytic cycle is a Pd(II)-Br complex coordinated with the reaction product ( $\eta^2$ -alkene and a bidentate directing group). The stability of this complex defines the overall energy span of the reaction. Co-catalyst KO<sub>2</sub>Piv plays a pivotal role by exchanging bromide for pivalate in the complex, via precipitation of the KBr coproduct. This removal of bromide from the reaction media decreases the energy span, avoiding the use of superstoichiometric silver salt reagents and allowing decooordination of the reaction product. In addition, pivalate facilitates the C(sp<sup>3</sup>)-H bond activation in the substrate once another substrate molecule is coordinated. The reaction conditions could be directly applied for (hetero)arylation given the weaker coordination of the reaction product, featuring a (hetero)aryl versus alkenyl and change in resting state. The picolinoyl directing group can be removed via amide esterification.

**KEYWORDS:** C-H activation, alkenylation, directing group, palladium catalysis, computational chemistry



## INTRODUCTION

In the past two decades, Pd-catalyzed C-H bond functionalization reactions have emerged as a novel tool for the formation of carbon-carbon and carbon-heteroatom bonds bringing potential advantages concerning step economy and waste reduction for organic synthesis.<sup>1</sup> In particular, the regioselective functionalization of C(sp<sup>2</sup>)-H bonds of arenes and heteroarenes has been extensively developed and widely adopted by synthetic organic chemists, whereas the corresponding selective functionalization of C(sp<sup>3</sup>)-H bonds of alkanes has, in comparison, been far less studied. In recent years, the Pd-catalyzed methodologies with the assistance of transition metal coordinating directing groups have shown tremendous progress toward the functionalization of remote ( $\beta$ ,  $\gamma$ , or  $\delta$ ) C(sp<sup>3</sup>)-H bonds, including aspects of regio- and stereoselectivity.<sup>1a-f</sup> Remarkably, among the various organohalide electrophiles used alkenyl halides have rarely been reported as reactants.<sup>2-4</sup> Moreover, these remote alkenylations of C(sp<sup>3</sup>)-H bonds all require superstoichiometric halide scavenging of silver reagents. With one exception,<sup>3e</sup> using a (*E*)- $\beta$ -bromostyrene, these are all limited to alkenyl iodides,

which are more expensive and less available than the corresponding bromides.<sup>1f</sup>

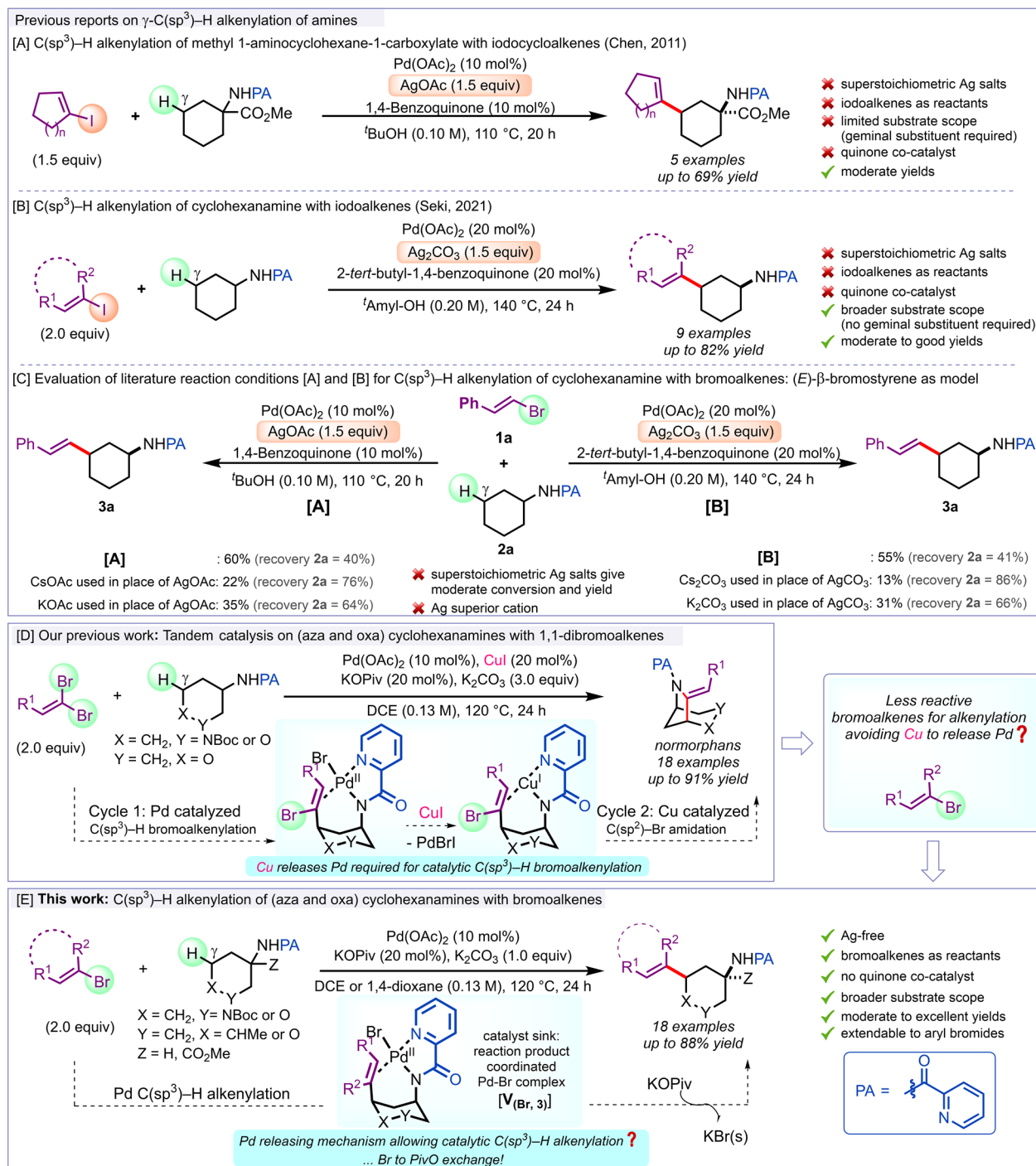
Aliphatic amines are found in chemical, pharmaceutical, textile, cosmetic, and metal industries. These chemicals are used as intermediates, solvents, rubber accelerators, catalysts, emulsifiers, synthetic cutting fluids, corrosion inhibitors, and flotation agents.<sup>5</sup> Considering their importance, the direct transformation of aliphatic amines via directed Pd-catalyzed C(sp<sup>3</sup>)-H bond functionalization has been studied over the past decade.<sup>6</sup> In particular, the easily removable and reusable picolinamide directing group is one of the powerful tools to achieve selective remote C(sp<sup>3</sup>)-H bond functionalization. In 2005, Daugulis and co-workers reported picolinamide directing group assisted Pd-catalyzed  $\gamma$ -C(sp<sup>3</sup>)-H arylation in aliphatic

**Received:** September 2, 2023

**Revised:** December 16, 2023

**Accepted:** December 17, 2023

**Scheme 1. Pd-Catalyzed  $\gamma$ -alkenylation of Cyclohexanamines Equipped with a Directing Group: State-of-the-Art Iodoalkenes (A, B), Application of the State-of-the-Art Conditions on Bromoalkenes (C), Our Previous Work with 1,1-Dibromoalkenes (D), and This Work with Bromoalkenes (E)**



amines with aryl iodides.<sup>7</sup> Since then, various functionalizations at remote sites in aliphatic amines have been reported, mainly using iodinated electrophiles, with methyl preference (concerted Pd-C bond formation: 1° > 2° > 3° alkyl-H).<sup>8</sup> Among these, the more difficult remote C(sp<sup>3</sup>)-H methylene bonds of cycloalkanamines are scarcely explored.<sup>6</sup> Remarkably, for the  $\gamma$ -C(sp<sup>3</sup>)-H alkenylation of cycloalkanamines, only two methods have been reported so far (Scheme 1).<sup>2</sup> The first method reported by Chen and co-workers is a Pd-catalyzed  $\gamma$ -C(sp<sup>3</sup>)-H alkenylation of methyl 1-picolinoylaminocyclohex-

ane-1-carboxylate, which employs cycloalkenyl iodides as alkenyl coupling partners and silver acetate reagent (Scheme 1A).<sup>2a</sup> The second method, reported by Seki and Takahashi, discloses a Pd-catalyzed  $\gamma$ -C(sp<sup>3</sup>)-H alkenylation of *N*-picolinoylcyclohexanamine employing alkenyl iodides as reactant and silver carbonate reagent (Scheme 1B).<sup>2b</sup> Both approaches are limited to alkenyl iodides as coupling partners and require a superstoichiometric silver salt reagent. Clearly, new and efficient silver-free reaction conditions are required based on alkenyl bromides. We recently developed a Pd and

Cu tandem catalytic process toward bridged bicyclic nitrogen scaffolds synthesis involving a Pd-catalyzed  $\gamma$ -C(sp<sup>3</sup>)-bromoalkenylation of *N*-picolinoylcyclohexanamine with 1,1-dibromoalkene, followed by a consecutive intramolecular Cu-catalyzed amidation of the 1-bromo-1-alkenylated intermediate.<sup>9</sup> Remarkably, the CuI required for the amidation step was shown to promote the Pd-catalyzed  $\gamma$ -C(sp<sup>3</sup>)-bromoalkenylation step of the tandem process by releasing intermediate product (i.e., 1-bromo-1-alkenylated) from the Pd catalyst via exchange with Cu (Scheme 1D). We disclose in this work  $\gamma$ -C(sp<sup>3</sup>)-H alkenylation of *N*-picolinoylcyclohexanamines with less reactive 1-bromoalkenes, lacking the geminal bromine atom under silver- and copper-free conditions relying on another Pd releasing mechanism (Scheme 1E).

The motivation to replace silver or cesium salts in state-of-the-art C–H functionalization protocols is based on price and the weight of the concomitant waste produced (Supporting Information, Sections S4 and S5). The abundance of metals in Earth's crust is generally reflected in the price of their corresponding inorganic salts (Figure 1 and Supporting

factors, potassium salts are preferred over silver and cesium salts.

In order to rationalize why no Ag salts are required in our alkenylation protocol, the reaction mechanism of the  $\gamma$ -C(sp<sup>3</sup>)-H functionalizations with organobromides was studied by using DFT calculations. Besides alkenyl bromide, aryl bromide was selected as a comparison. The catalytic cycle proposed for the Pd(II) catalyzed C–H functionalization reactions with electrophilic coupling partners typically goes through Pd(II)/Pd(IV) pathways.<sup>6</sup> Previous computational studies on these reactions have focused on the mechanism of the C–H bond activation step and other selected reaction steps to address aspects like stereoselectivity,<sup>10</sup> the formation of crucial off-cycle Pd species,<sup>11</sup> or competitive  $\beta$ -hydride elimination reactions.<sup>12</sup> However, few computational studies have looked at the full catalytic cycle, and these studies involve C(sp<sup>2</sup>)-H bonds<sup>10f,13</sup> or the use of organoiodide reactants.<sup>11,14</sup> In the case of C(sp<sup>3</sup>)-H and organobromide coupling partners, it is difficult to predict whether the C–H bond activation or the organobromide addition to Pd(II) would be the rate limiting step.<sup>6a,15</sup> In this work, we disclose that for  $\gamma$ -C(sp<sup>3</sup>)-H functionalization of cyclohexanamines with alkenyl bromides, the C–H bond activation involves the highest energy barrier. The lowest energy complex in the catalytic cycle is a Pd(II)-Br complex coordinated to the reaction product [V<sub>(Br,3)</sub>]. For strongly coordinating reaction products containing a C=C bond and directing group, this resting state complex V<sub>(Br,3)</sub> becomes a catalyst sink and a limiting factor for the turnover of the C(sp<sup>3</sup>)-H functionalization reaction, requiring an effective transformation into a more reactive Pd complex.

## RESULTS AND DISCUSSION

**C(sp<sup>3</sup>)-H Alkenylation of (Aza- and Oxa-) Cyclohexanamines with Bromoalkenes.** We began our investigation of the  $\gamma$ -C(sp<sup>3</sup>)-H alkenylation of cyclohexanamines with *N*-picolinoylcyclohexanamine (2a) and (*E*)- $\beta$ -bromostyrene (1a) as model coupling partners. When we applied the two sets of conditions reported for the  $\gamma$ -C(sp<sup>3</sup>)-H alkenylation of *N*-picolinoylcyclohexanamine with iodoalkenes on the model system, moderate conversion (~60%) and product yields (55–60%) were obtained (Scheme 1C, and Supporting Information Section S2). Furthermore, when we replaced silver salts with either cesium or potassium salts, lower conversion and product yields were obtained in accordance with the superior halide scavenging role of silver (Scheme 1C).<sup>1g,h</sup> When applying our

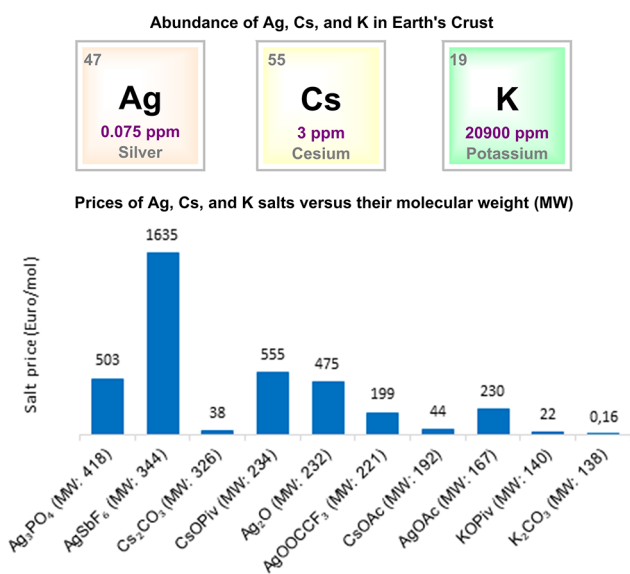


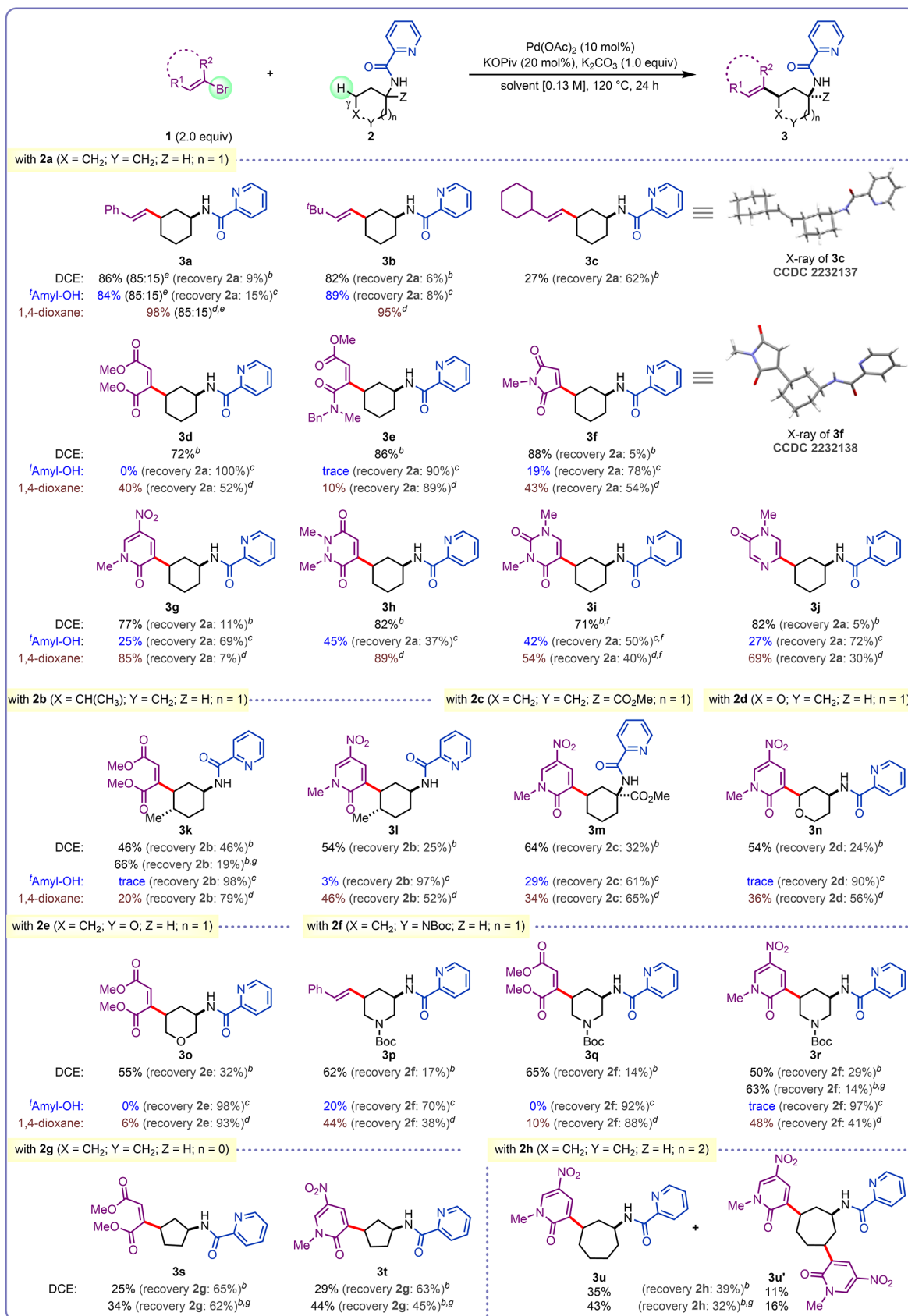
**Figure 1.** Prices of Common Reagents and the cation abundances of their reagents in Earth's Crust. MW = molecular weight.

Information Section S6.2), and the higher molecular weight of the metal, the more waste (in g) is produced. Based on both

**Table 1.** Reaction Optimization on the Model Reaction of (*E*)- $\beta$ -Bromostyrene (1a) with *N*-Picolinoylcyclohexanamine (2a)

| entry | deviation from standard conditions                     | reaction time, h | recovery of 2a, % <sup>a</sup> | yield of 3a, % <sup>a</sup> |
|-------|--|------------------|--------------------------------|-----------------------------|
| 1     | with 20 mol % CuI                                      | 24               | 14                             | 79                          |
| 2     | none   | 24               | 11 (9) <sup>b</sup>            | 89 (86) <sup>b</sup>        |
| 3     | absence of KOPIv                                       | 24               | 55                             | 45                          |
| 4     | absence of K <sub>2</sub> CO <sub>3</sub>              | 24               | 78                             | 11                          |
| 5     | ( <i>E</i> )- $\beta$ -iodostyrene used in place of 1a | 24               | 1 (1) <sup>b</sup>             | 98 (94) <sup>b</sup>        |

<sup>a</sup><sup>1</sup>H NMR yield. *cis* major compound see Supporting Information Table S3–S4. <sup>b</sup>Isolated yield.

Scheme 2. Scope of the Diastereoselective Pd-Catalyzed  $\gamma$ -C(sp<sup>3</sup>)-H Alkenylation with Bromoalkenes<sup>a</sup>

<sup>a</sup>Full *cis* diastereoselectivity except for 3a. When no recovery of 2 is indicated, it was <5%. <sup>b</sup>1,2-Dichloroethane used as solvent. Isolated yields. <sup>c</sup>*tert*-Amyl alcohol used as solvent. <sup>d</sup><sup>1</sup>H NMR yields. <sup>e</sup>1,4-Dioxane used as solvent. <sup>f</sup><sup>1</sup>H NMR yields. <sup>g</sup>*Cis/trans* ratio. <sup>h</sup>5.0 equiv of bromoalkene was used. <sup>i</sup>20 mol % Pd(OAc)<sub>2</sub> was used.

previously reported reaction conditions optimized for  $\beta,\beta$ -bromostyrene as the electrophile, in the framework of the tandem protocol toward normorphans (Scheme 1D), the targeted  $\gamma$ -alkenylated cyclohexanamine, i.e., 3-(2-phenylethenyl)-*N*-picolinoylcyclohexanamine (**3a**) was obtained in 79% yield with 14% recovery of **2a** (Table 1, entry 1).<sup>9</sup> **1a** lacks a bromine atom versus  $\beta,\beta$ -bromostyrene and is, therefore, less reactive versus oxidative addition. When omitting catalytic CuI, a better mass balance and 89% **3a** was obtained (Table 1, entry 2), indicating an inhibiting rather than a promoting role for this additive when only C–H alkenylation is involved and no tandem bromoalkenylation–amidation reaction. Deviation from these conditions indicated which parameters are crucial in the  $\gamma$ -alkenylation process (Table 1, and Supporting Information Section S3). Omitting the additive KOPiv or performing the reaction in the absence of K<sub>2</sub>CO<sub>3</sub> furnished conversions of less than 50% and low yields of **3a**, 45 and 11%, respectively (Table 1, entries 3 and 4). The use of (*E*)- $\beta$ -iodostyrene (**1aa**) in place of (*E*)- $\beta$ -bromostyrene yielded the desired product **3a** in 98% yield (entry 5), also without using silver additives which are required with iodinated coupling partners (Scheme 1A,B).

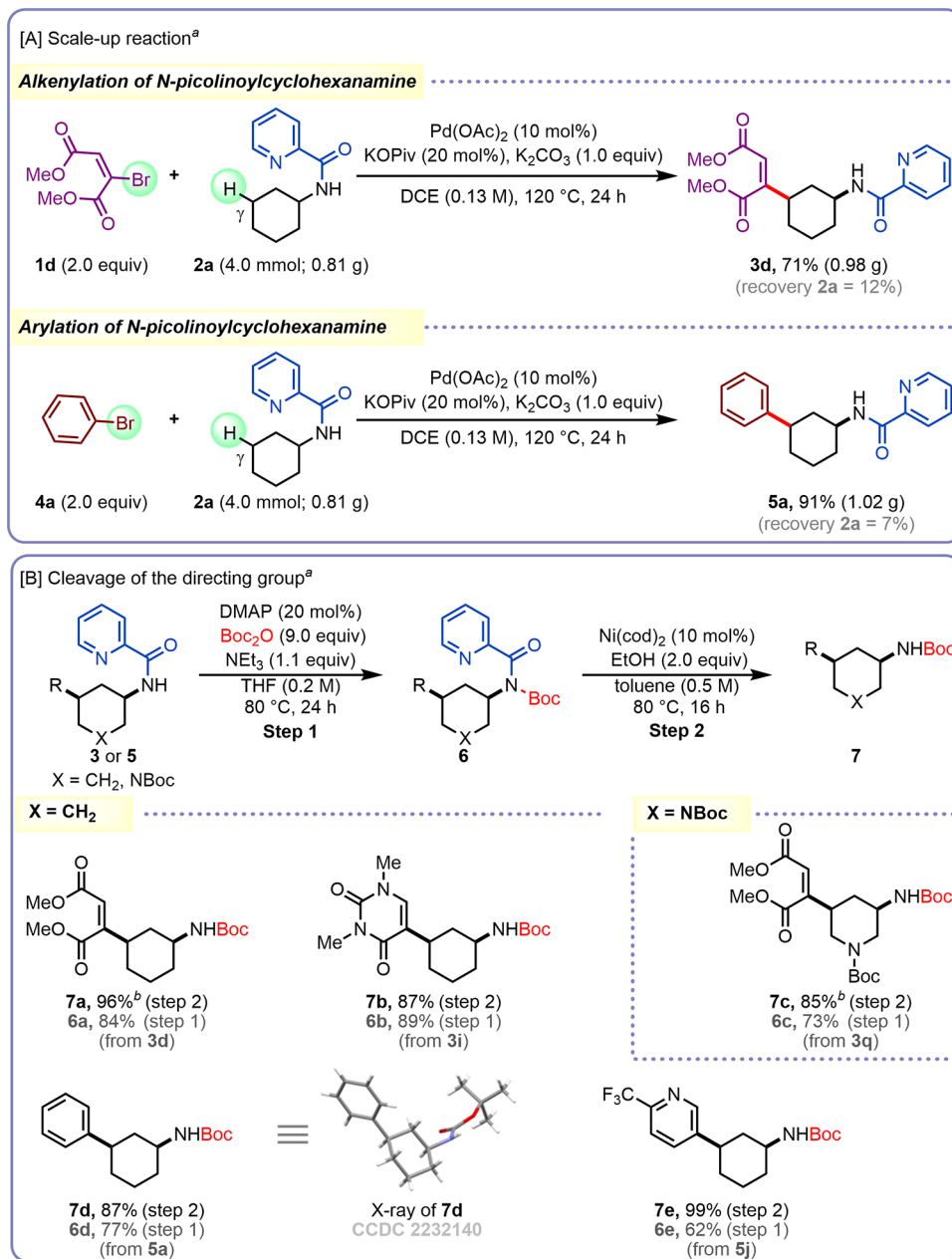
Encouraged by the outcome of the  $\gamma$ -C(sp<sup>3</sup>)–H alkenylation of **2a** with (*E*)- $\beta$ -bromostyrene (**1a**), we next evaluated the bromoalkene scope with more challenging coupling partners **1**, which are not styrene based (Scheme 2). Interestingly, aliphatic bromoalkenes (*E*)-1-bromo-3,3-dimethylbut-1-ene (**1b**) and (*E*)-(2-bromovinyl)cyclohexane (**1c**) provided the desired reaction products. While the former gave 94% conversion of **2a** and 82% yield of **3b**, the latter gave 27% **3c** and 62% recovered **2a**. Esters and amide conjugated with the double bond were well tolerated as illustrated with coupling partners dimethyl 2-bromomaleate (**1d**) and methyl (*E*)-4-[benzyl(methyl)amino]-3-bromo-4-oxobut-2-enoate (**1e**), providing high yields of **3d** and **3e**, in 72 and 86%, respectively. The double bond can also be included in an imide, as shown by the efficient coupling with 3-bromo-1-methyl-1*H*-pyrrole-2,5-dione (**1f**). Interestingly, azinones [3-bromo-1-methyl-5-nitropyridin-2(1*H*)-one (**1g**)] as well as diazinones [4-bromo-1,2-dimethyl-1,2-dihydropyridazine-3,6-dione (**1h**), 5-bromo-1,3-dimethyluracil (**1i**), and 5-bromo-1-methylpyrazin-2(1*H*)-one (**1j**)] proved also suitable coupling partners with **2a**, and the desired corresponding alkenylated products **3g**, **3h**, **3i**, and **3j** were obtained in high yields. The cyclohexanamine can also be substituted in the position next to the methylene, as exemplified by the reaction of *trans*-4-methyl-*N*-picolinoylcyclohexanamine (*trans*-**2b**) with **1d** and **1g**, delivering the alkenylated product **3k** and **3l** in moderate yields (46 and 54%, respectively) without altering the reaction conditions. Unnatural amino acid ester **2c** reacted with bromopyridin-2(1*H*)-one **1g**, delivering alkenylated product **3m** in 64% yield. To our delight, also oxa- and aza- analogues of cyclohexanamines, i.e., *N*-picolinoyltetrahydro-2*H*-pyran-4-amine (**2d**), *N*-picolinoyltetrahydro-2*H*-pyran-3-amine (**2e**), and 1-Boc-*N*-picolinoyl-piperidin-3-amine (**2f**), provided target compounds under the standard reaction conditions, further supporting its generality. The reaction of **2d** with bromopyridin-2(1*H*)-one **1g** furnished the corresponding desired product **3n** in 54% yield. The reaction of **2e** with 2-bromomaleate **1d** also gave the corresponding desired product

**3o** in 55% yield. Starting material **2f** reacted with bromostyrene **1a**, bromomaleate **1d**, and bromopyridin-2(1*H*)-one **1g**, affording the desired alkenylated products **3p**, **3q**, and **3r** in 62, 65, and 50% yields, respectively. With these challenging substituted and heterocyclic substrates,<sup>16</sup> starting materials **2b–f** were easily recycled under the standard conditions. However, the mass balances were high, indicating the high chemoselectivity of the reaction. Alternative solvents were also studied. *t*-Amyl alcohol generally proved to be a poor solvent, particularly for alkenylation reactions featuring heteroatom containing **2** and/or **1** (Scheme 2). Interestingly, 1,4-dioxane gave better results with the exception of the diester (**1d**) or mixed ester/amide (**1e**) of bromomaleic acid as reactants providing poor yields of the corresponding reaction products. Bromo(di)azinones **1g–j** performed equally well in comparison to DCE though with challenging substrates **2** (C-substituted and aza- and oxa cyclohexanamines, **2b–f**) with lower conversions and yields. This methodology could also be extended to five- and seven-membered cycloalkylamine substrates, without adaptation of the reaction conditions, as exemplified by the reaction of *N*-picolinoylcyclopentanamine (**2g**) with **1d** and **1g**, and the reaction of *N*-picolinoylcycloheptanamine (**2h**) with **1g** under standard conditions, giving the desired alkenylation products **3s**, **3t**, and **3u** in moderate yields (Scheme 2). Interestingly, in the case of seven-membered cyclic amine substrate **2h** under these conditions, 11% of dialkenylation product **3u'** was isolated which was never detected on other substrates **2**. For the different substrates (*trans*-**2b**, **2f**, **2g**, **2h**) an example with moderate conversion with bromoalkene **1d** and/or **1g** was selected and repeated with a double loading of Pd(OAc)<sub>2</sub> (20 mol %). However, the yields of **3k**, **3r**, **3s**, **3t**, and **3u** were only slightly improved (8–20% yields).

**C(sp<sup>3</sup>)–H Arylation of (Aza- and Oxa-) Cyclohexanamines with (Hetero)aryl Bromides.** Inspired by the results with bromo(di)azinones, we wondered whether the reaction conditions could also allow  $\gamma$ -C(sp<sup>3</sup>)–H arylation of the same substrates (**2**) employing aryl bromides (**4**) rather than bromoalkenes (**1**) as a coupling partner (Scheme 3). We reasoned that the incorporation of the double bond into an aromatic system will impact the energy of several steps in the reaction mechanisms and therefore provide a good comparison for the DFT studies (*vide infra*). Gratifyingly, bromobenzene (**4a**) reacted with *N*-picolinoylcyclohexanamine (**2a**) under our reaction conditions without any alteration, providing 99% 3-phenyl-*N*-picolinoylcyclohexanamine (**5a**). Interestingly, aryl bromides bearing both electron-donating [i.e., methoxy (**4b**)] and electron-withdrawing [chloro (**4c**), ester (**4d**), trifluoromethyl (**4e**), cyano (**4f**), and nitro (**4g**)] groups were also compatible under the standard reaction conditions providing the corresponding  $\gamma$ -C(sp<sup>3</sup>)–H arylated products **5b–5g** in 77–89% yield. In addition, heteroaryl bromides such as 2-bromofuran (**4h**), 2-bromothiophene (**4i**), 5-bromo-2-(trifluoromethyl)pyridine (**4j**), regioisomeric 2-bromo-6-(trifluoromethyl)pyridine (**4k**), 3-bromo-1-(phenylsulfonyl)-1*H*-indole (**4l**), and 6-bromoquinoxaline (**4m**) also provided good to excellent yields of the corresponding arylation products (**5h** in 79%, **5i** in 84%, **5j** in 86%, **5k** in 88%, **5l** in 66%, and **5m** in 89% isolated yield). The cyclohexanamine can also be substituted in the position next to the methylene, as



Scheme 4. (A) Gram-Scale Reaction and (B) Cleavage of the Picolinoyl Directing Group

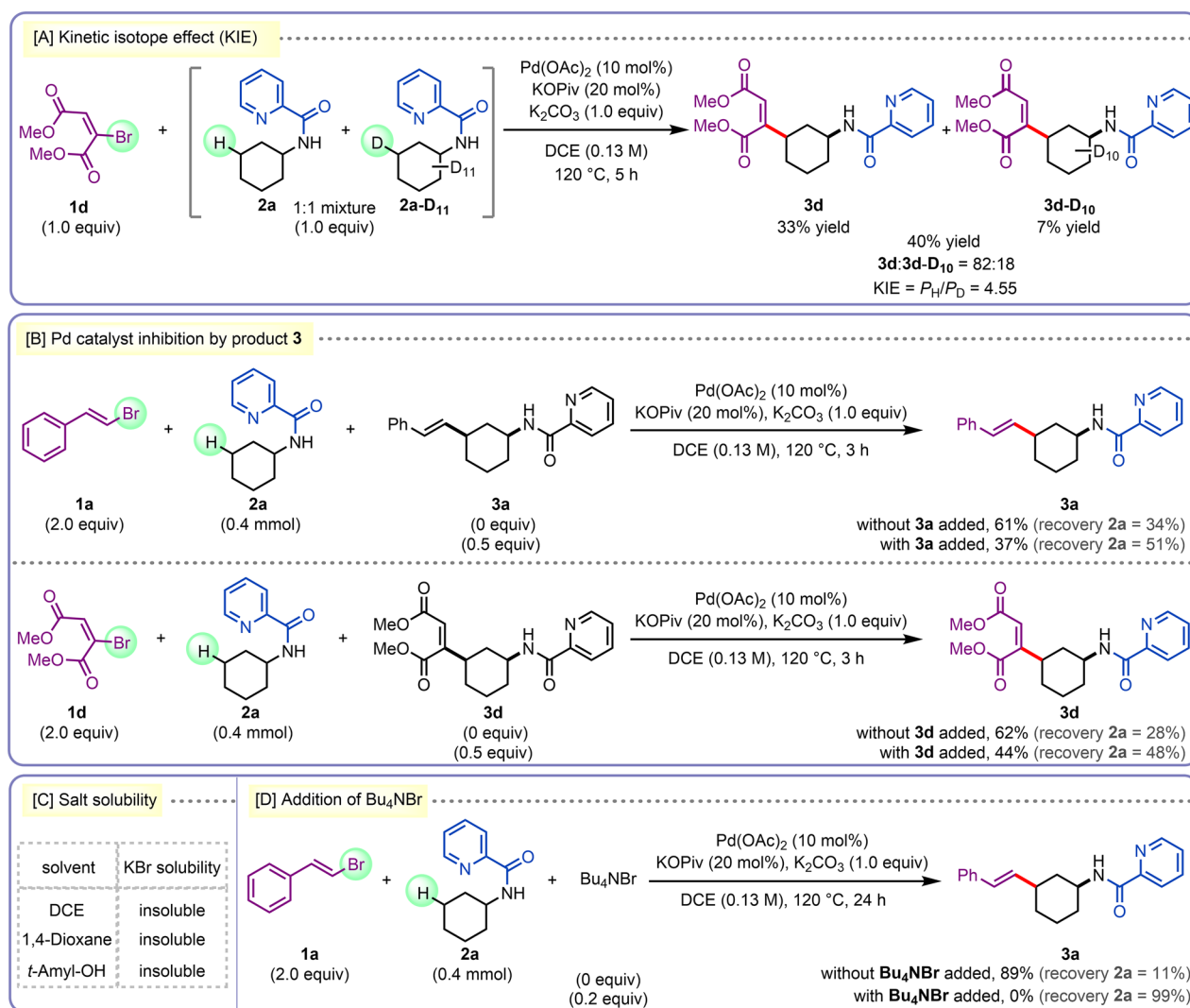


<sup>a</sup>Isolated yield. <sup>b</sup>MeOH (5.0 equiv) was used in place of EtOH (2.0 equiv). DMAP = 4-dimethylaminopyridine.

exemplified by the reaction of *trans*-4-methyl-*N*-picolinoylcyclohexanamine (*trans*-**2b**) with bromobenzene (**4a**) and 5-bromo-2-(trifluoromethyl)pyridine (**4j**), delivering the arylated products **5n** and **5o** in moderate yields (65 and 63%, respectively). Unnatural amino acid ester **2c** performed similarly as **2a** in an arylation with 1-bromo-4-methoxybenzene (**4b**) and 1-bromo-4-nitrobenzene (**4g**) providing the desired products **5p** and **5q** in good yields. Remarkably, in this case a low percentage (10–15%) of 3,5-diarylation was also observed, which was never detected on other substrates **2**. Notably, also heterocyclic analogues of cyclohexanamine can be applied without altering the standard conditions. The reaction of bromobenzene (**4a**) and 4-bromoanisole (**4b**) with *N*-picolinoyltetrahydro-2*H*-pyran-4-amine (**2d**) delivered the corresponding (hetero)arylated products **5r** and **5s** in excellent yields. The reaction of regioisomeric *N*-picolinoyltetrahydro-

2*H*-pyran-3-amine (**2e**) with bromobenzene (**4a**) and 5-bromo-2-(trifluoromethyl)pyridine (**4j**) delivered the corresponding arylated products **5t** and **5u** in good yields, though with some remaining substrate. Aza analogue 1-Boc-*N*-picolinoylpiperidin-3-amine (**2f**) performed equally well (**5v** and **5w** in 61 and 64% yields, respectively). Alternative solvents were also studied. *t*-Amyl alcohol generally proved to be a good solvent with some exceptions (**5f**, **5h**, and **5m**), though lower conversions than in DCE were obtained for challenging substrates **2** (C-substituted and aza and oxa cyclohexanamines, **2b–f**). When five- and seven-membered cycloalkanamine substrates **2g** and **2h** were subjected to the standard reaction conditions, the desired arylation products **5x**, **5y**, and **5z** were obtained in moderate yields (Scheme 3). However, in the case of *N*-picolinoylcycloheptanamine substrate **2h** under these conditions, 16% of diarylation

**Scheme 5. Control Reactions to Support the Catalytic Cycle: (A) Kinetic Isotope Effect (KIE); (B) Pd Catalyst Inhibition by Product 3; (C) Salt Solubility; (D) Addition of Bu<sub>4</sub>NBr**



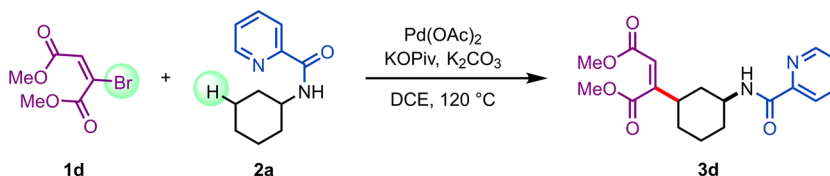
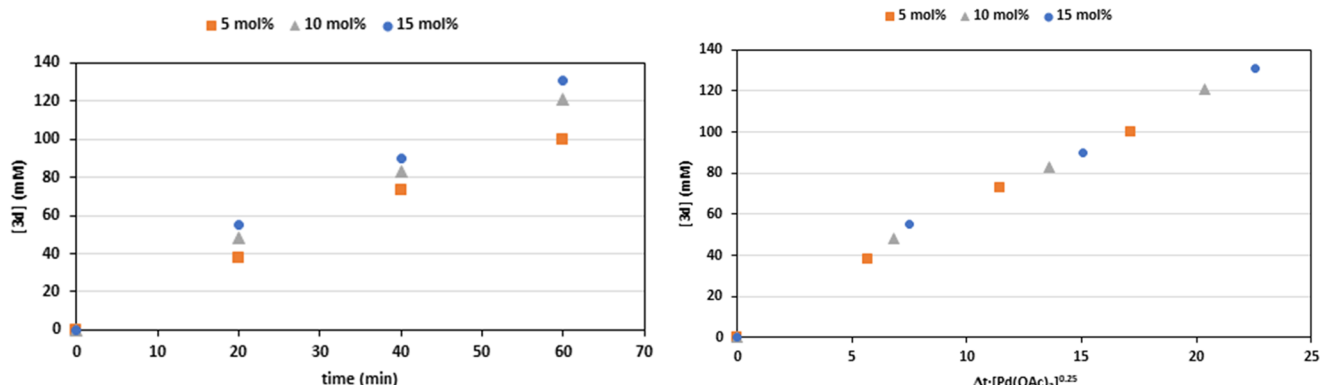
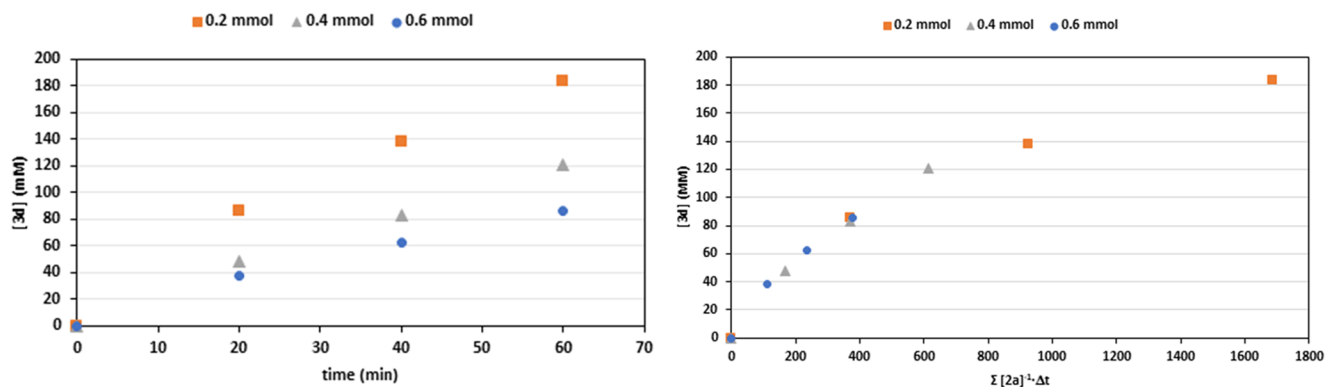
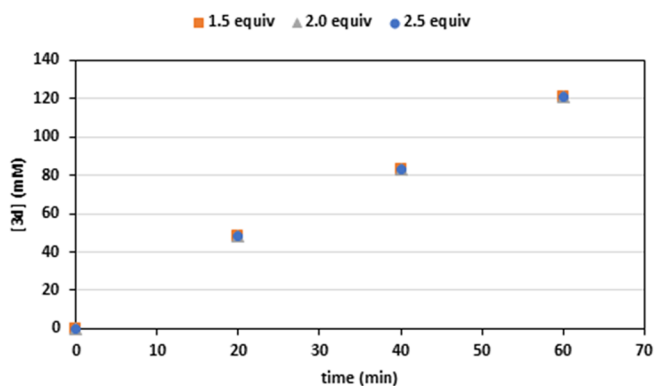
product **5z'** was isolated in addition to the monoarylation product **5z**. This is similar to what was observed in the  $\gamma$ -C(sp<sup>3</sup>)-H alkenylation (*vide supra*).

**Diastereoselectivity.** Full *cis*-diastereoselectivity was obtained in all of the  $\gamma$ -C(sp<sup>3</sup>)-H alkenylation (**3**) and arylation (**5**) reactions imposed by the reaction mechanism of the C-H activation step (*vide supra*) with the exception of 3-(2-phenylethenyl)-*N*-picolinoylcyclohexanamine (**3a**). By subjecting reaction product **3a** to the same reaction conditions of the functionalization, we could prove that this is a Pd-catalyzed postisomerization of the *cis* diastereoisomer as the *cis:trans* ratio changed from 87:13 to 76:24 (Supporting Information, Scheme S4). This is presumably due to the activated nature of the cinnamyl moiety. Also, the double bond geometry of reactants **1** was fully retained in all of the reaction products **3**.

**Reaction Scalability and Removal of the Directing Group.** Scale-up experiments were performed for showcasing the scalability of our alkenylation and arylation methods (Scheme 4A). Scaling up the reaction 10-fold to 4 mmol of *N*-picolinoylcyclohexanamine (**2a**) with coupling partners dimethyl 2-bromomaleate (**1d**) and bromobenzene (**4a**) delivered the desired products **3d** and **5a** in 71 and 91% yields, respectively. Next, we focused our attention on the

removal of the picolinoyl directing group. In this regard, we applied our previously developed two-step method for the cleavage of the picolinamide directing group *via* *N*-Boc activation followed by Ni-catalyzed esterification with alcohol on both alkenylated (**3d**, **3i**, and **3q**) and arylated (**5a** and **5j**) products (Scheme 4B).<sup>17,18</sup> Boc activation of **3** and **5** with (Boc)<sub>2</sub>O in THF at 80 °C for 24 h gave the resulting Boc products **6** in good to excellent isolated yields. Next, these Boc-protected picolinamides were treated with Ni(cod)<sub>2</sub> (10 mol %) and ethanol (2.0 equiv) in toluene at 80 °C for 16 h, which delivered the corresponding Boc protected amines **7** in excellent isolated yields. In the case of alkenylated substrates derived from dimethyl bromomaleate, methanol (5.0 equiv) is used instead of ethanol to avoid the transesterification in the resulting reaction products.

**Study of the Reaction Mechanism.** To gain insight into the reaction mechanism, the kinetic isotope effect (KIE) was determined. A competitive experiment with equimolar amounts of *N*-picolinoylcyclohexanamine (**2a**) and **2a-D**<sub>11</sub> in a reaction with dimethyl 2-bromomaleate (**1d**) gave a KIE value of 4.55, which suggests that the C(sp<sup>3</sup>)-H bond cleavage is the rate-determining step in this reaction (Scheme 5A and Supporting Information Section S9). Furthermore, kinetic

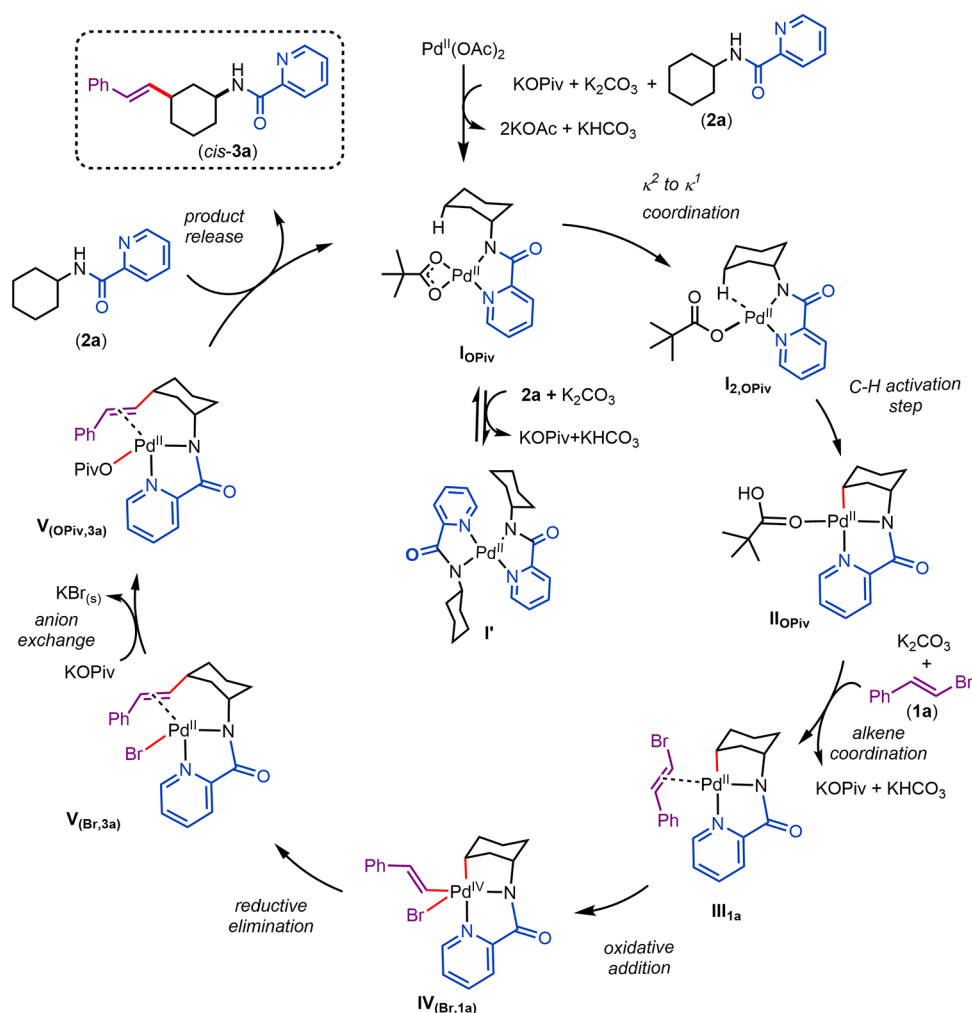
[A] 0.25 Order in  $\text{Pd}(\text{OAc})_2$ [B] -1<sup>st</sup> Order in amide **2a**[C] 0 Order in bromoalkene **1d**

**Figure 2.** Use of VTNA to determine the reaction order in  $\text{Pd}(\text{OAc})_2$ , amide **2a**, and bromoalkene **1a**. The profiles obtained under standard conditions are represented by gray triangles. Left column: concentration of product **3d** as a function of time using different initial concentrations of (A)  $\text{Pd}(\text{OAc})_2$ , (B) amide **2a**, and (C) bromoalkene **1d**. Right column: concentration profiles of **3d** after time scale normalization for a 0.25 order in (A)  $\text{Pd}(\text{OAc})_2$ , for a  $-1$  order in (B) amide **2a**, and for a zero order in (C) bromoalkene **1d**. Reaction conditions: (a) **2a** (0.4 mmol), bromoalkene **1d** (0.8 mmol),  $\text{Pd}(\text{OAc})_2$  (0.02–0.06 mmol),  $\text{KOPiv}$  (0.08 mmol),  $\text{K}_2\text{CO}_3$  (0.4 mmol),  $\text{DCE}$  (3 mL),  $120\text{ }^\circ\text{C}$ ; (b) **2a** (0.2–0.6 mmol), bromoalkene **1d** (0.8 mmol),  $\text{Pd}(\text{OAc})_2$  (0.04 mmol),  $\text{KOPiv}$  (0.08 mmol),  $\text{K}_2\text{CO}_3$  (0.4 mmol),  $\text{DCE}$  (3 mL),  $120\text{ }^\circ\text{C}$ ; (c) **2a** (0.4 mmol), bromoalkene **1d** (0.6–1.0 mmol),  $\text{Pd}(\text{OAc})_2$  (0.04 mmol),  $\text{KOPiv}$  (0.08 mmol),  $\text{K}_2\text{CO}_3$  (0.4 mmol),  $\text{DCE}$  (3 mL),  $120\text{ }^\circ\text{C}$ . Each data point corresponds to a discrete reaction.

analysis of the same reaction using variable time normalization analysis (VTNA)<sup>14e,19</sup> revealed a 0.25 order in  $\text{Pd}(\text{OAc})_2$ , a  $-1$

order in amide **2a**, and a zero-order in bromoalkene **1d** (Figure 2 and Supporting Information Section S10). To rationalize the

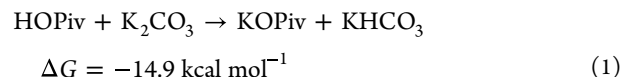
**Scheme 6. Computed Reaction Mechanism for the  $\gamma$ -C(sp<sup>3</sup>)-H Alkenylation of *N*-Picolinoylcyclohexanamine (2a) with (*E*)- $\beta$ -bromostyrene (1a) as the Model Reaction Studied by DFT**



KIE and kinetic results, the reaction mechanism of the Pd-catalyzed  $\gamma$ -C(sp<sup>3</sup>)-H alkenylation of cyclohexanamines was also investigated computationally through density functional theory (DFT, M06-D3/def2-SVP//def2-TZVP, SMD)<sup>20</sup> calculations using (*E*)- $\beta$ -bromostyrene (1a) and *N*-picolinoylcyclohexanamine (2a) as model reactants.

**Catalytic Cycle.** The reaction mechanism of the entire catalytic cycle and the corresponding Gibbs free energy profile diagram are shown in Scheme 6 and Figure 3, respectively. A possible Pd(0)/Pd(II) pathway was studied but disregarded due to high energy barriers (Supporting Information Scheme S8). In the first step of the reaction mechanism, the catalyst precursor Pd(OAc)<sub>2</sub> is transformed into the catalytically active Pd(II) species IOPIv by reaction with the substrate *N*-picolinoylcyclohexanamine (2a), KOPIv and K<sub>2</sub>CO<sub>3</sub>, which are present in larger concentrations than the released KOAc. This step is a highly exergonic process with  $\Delta G = -31.0$  kcal mol<sup>-1</sup>, suggesting a strong interaction of Pd(II) with reactant 2a. The coordination and deprotonation of a second substrate molecule yielding I' and byproducts KOPIv and KHCO<sub>3</sub> is also exergonic, but in a lower extent ( $\Delta G = -8.6$  kcal mol<sup>-1</sup>). This species I' is in equilibrium with the catalytically active IOPIv complex, which explains the order -1 in substrate obtained experimentally. It is important to notice that these reactions (formation of IOPIv and I' from Pd<sup>II</sup>(OAc)<sub>2</sub>), and

others described later, are highly driven by the deprotonation of the HOPiv byproduct by K<sub>2</sub>CO<sub>3</sub> as shown in eq 1, which will be highly influenced by the solubility of the involved salts. The absence of this deprotonation reaction would make the formation of I' from IOPIv endergonic by 6.3 kcal mol<sup>-1</sup>.



Following the formation of IOPIv, the C(sp<sup>3</sup>)-H bond of the coordinated substrate is broken via a concerted metalation deprotonation (CMD) pathway, consistent with previous mechanistic studies providing II<sub>OPiv</sub>.<sup>21</sup> In this step, the proton is transferred to the coordinated pivalate, via a six-membered ring transition state TSI<sub>OPiv</sub>, which has an energy of 25.1 kcal mol<sup>-1</sup> above IOPIv, and 33.7 kcal mol<sup>-1</sup> above I'. The latter energy barrier is *ca* 1 kcal mol<sup>-1</sup> higher than expected for the experimental conditions, which is reasonable considering the errors associated with DFT and omitting solubility issues. The transformation goes via a Pd(II) C-H agostic intermediate I<sub>2,OPiv</sub> allowed by a change in the pivalate coordination from  $\kappa^2$  to  $\kappa^1$ . As a consequence of the agostic interaction, the C(sp<sup>3</sup>)-H bond distance increases from 1.10 (in IOPIv) to 1.14 Å (in I<sub>2,OPiv</sub>), facilitating subsequent C-H bond cleavage. Next, the substitution of the protonated pivalic acid (HOPiv) in II<sub>OPiv</sub> by

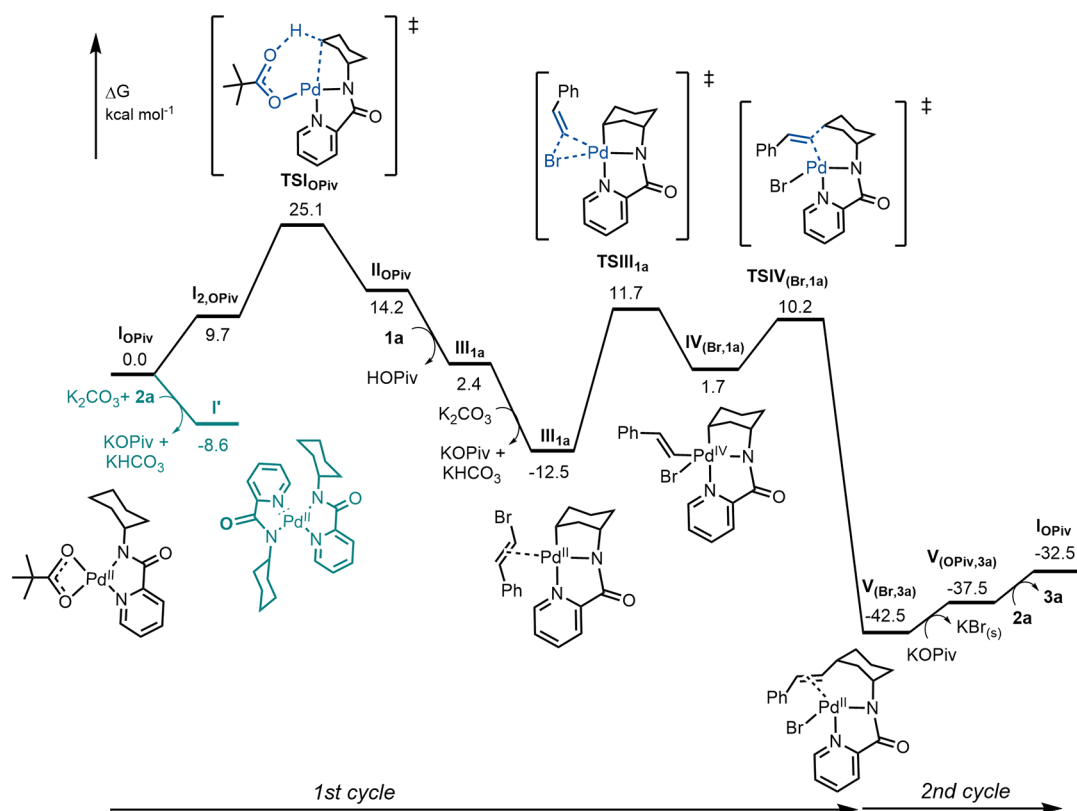


**Figure 3.** Energy diagram for the  $\gamma$ -C(sp<sup>3</sup>)-H alkenylation of *N*-picolinoylcyclohexanamine (**2a**) with (*E*)- $\beta$ -bromostyrene (**1a**) as a model reaction studied by DFT.

(*E*)- $\beta$ -bromostyrene (**1a**) and HOPIV deprotonation by K<sub>2</sub>CO<sub>3</sub> is highly exergonic ( $\Delta G = -26.7$  kcal mol<sup>-1</sup>, see also eq 1) yielding  $\eta^2$ -alkene coordinated intermediate III<sub>1a</sub>. This reaction makes the overall C–H bond activation an irreversible process, in line with the KIE observed. In a subsequent oxidative addition, the palladium center is oxidized from Pd(II) to Pd(IV) with an activation barrier of 24.2 kcal mol<sup>-1</sup>, yielding IV<sub>(Br,1a)</sub>. Generally, Pd(IV) intermediates are highly unstable compared to Pd(II). However, the strong  $\sigma$  donation of the amide ligand to the palladium center stabilizes the Pd(IV) species.<sup>22</sup> This effect is consistent with the large stabilization energy (SE = 117.5 kcal mol<sup>-1</sup>) obtained for this interaction as determined by natural bond orbital (NBO) analysis.<sup>23</sup> For comparison, the SE for the  $\sigma$  donation of pyridine to Pd(IV) was found to be 38.1 kcal mol<sup>-1</sup> (Supporting Information Figure S3). The insertion of bromoalkene **1a** into the Pd–C(sp<sup>3</sup>) bond<sup>24</sup> was also investigated as an alternative pathway to the oxidative addition. However, the transition state associated with this pathway (TSIII<sub>Ins</sub>) is 10.4 kcal mol<sup>-1</sup> higher in energy than TSIII<sub>1a</sub> (Supporting Information Figure S5B) ruling this possibility out. In a subsequent reaction step, the C–C bond formation takes place via reductive elimination yielding V<sub>(Br,3a)</sub>, in which the oxidation state of palladium is reduced to +2. This step is expected to be fast (activation barrier of 8.5 kcal mol<sup>-1</sup>), and highly exergonic ( $\Delta G = -44.2$  kcal mol<sup>-1</sup>). The high stability of V<sub>(Br,3a)</sub> turns this intermediate into the resting state of the catalytic cycle. As shown in Figure 3, going back to I<sub>OPiv</sub> by product **3a** release and formation of KBr costs 10.0 kcal mol<sup>-1</sup>, which results in an overall energy span<sup>25</sup> of 35.1 kcal mol<sup>-1</sup>, which is too high to be overcome at 120 °C. However, we found KBr is insoluble in DCE (Scheme 5C, Supporting

Information, Section 7). This drives the reaction toward V<sub>(OPiv,3a)</sub>, hereby decreasing the energetic span to 30.1 kcal mol<sup>-1</sup>, which is reasonable under the experimental conditions. These results suggest that both the solvent and the KOPIV additive play a crucial role in this reaction: the solvent by removing the bromide anions by precipitation of KBr and the pivalate by destabilizing the Pd resting state (V<sub>Br,3a</sub> to V<sub>OPiv,3a</sub>), hereby decreasing the overall energy barrier for the C–H bond cleavage. This rationalizes why alkenylation reactions are particularly challenging to develop and alkenyl halides have rarely been reported as reactants and required silver halide scavengers. While KBr is not soluble in DCE, *t*-amyl alcohol, and 1,4-dioxane (Scheme 5C, Supporting Information Section S7), therefore potentially suitable solvents for the crucial Br exchange in V<sub>(Br,3)</sub> by OPiv, DCE proved to be a more general solvent (Scheme 2). Likely, the lack of specific interactions (no Lewis basicity and hydrogen bonding) and high solvating ability of DCE are responsible.

#### Effect of Anion X on the C(sp<sup>3</sup>)-H Bond Activation Step.

The proton transfer in the CMD mechanism of the C(sp<sup>3</sup>)-H activation can involve different anions than pivalate (OPiv) present in the KOPIV additive, i.e., acetate (OAc), bicarbonate (HCO<sub>3</sub>), and bromide (Br) also present in the reaction mixture. Acetate was considered as it appears in the Pd(OAc)<sub>2</sub> precatalyst added. Bicarbonate is formed in the reaction, considering that K<sub>2</sub>CO<sub>3</sub> is the stoichiometric base used. Bromide is the leaving group of electrophile **1a**. Interestingly, also bromide can induce the C(sp<sup>3</sup>)-H activation,<sup>21f,26</sup> forming HBr. In Figure 4, an overview of the energy diagram of this step is given. In agreement with the literature,<sup>26</sup> the energetic span V<sub>(X,3a)</sub> → TSI<sub>X</sub> is highest for X = Br with 38.8 kcal mol<sup>-1</sup> so this pathway will certainly not play a role here.

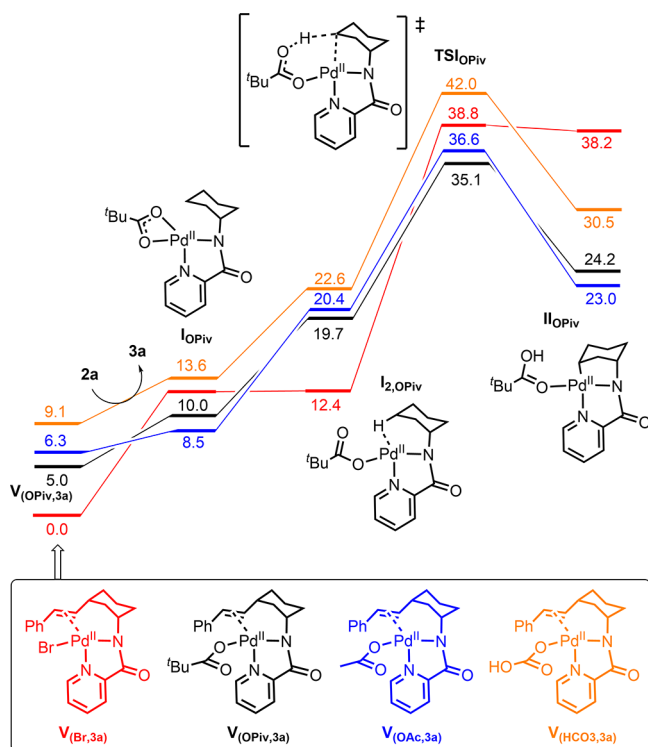


**Figure 4.** Effect of anion for Pd(II) in the Gibbs free energy profile for the C(sp<sup>3</sup>)-H activation in *N*-picolinoylcyclohexanamine (**2a**). Gibbs free energies in kcal mol<sup>-1</sup>.

However, with X = HCO<sub>3</sub> the energetic span decreases to 32.9 kcal mol<sup>-1</sup> and further decreases to around 30 kcal mol<sup>-1</sup> for X = OPiv, OAc. These results indicate that carboxylates are required to destabilize the bromide complex V<sub>(Br,3a)</sub> besides their role in the C(sp<sup>3</sup>)-H activation mechanism. In accordance with this, when the KO<sub>2</sub>Piv additive was omitted in the  $\gamma$ -C(sp<sup>3</sup>)-H alkenylation of *N*-picolinoylcyclohexanamine (**2a**) with (*E*)- $\beta$ -bromostyrene (**1a**), the yield dropped from 89 to 45% (Table 1, entries 2 and 3). Moreover, addition of 20 mol % Bu<sub>4</sub>NBr completely blocked catalysis as pivalate coordination to Pd(II) is blocked (Scheme 5D).

**Effect of the Electrophile RX on the Oxidative Addition and Catalyst Resting State.** The energy profile depicted in Figure 3 shows that for the reactants (*E*)- $\beta$ -bromostyrene (**1a**) and *N*-picolinoylcyclohexanamine (**2a**), the highest energy barrier of the catalytic cycle corresponds to the C(sp<sup>3</sup>)-H bond activation step. Therefore, the oxidative addition of (*E*)- $\beta$ -bromostyrene to Pd(II), which has an energy barrier of 24.2 kcal mol<sup>-1</sup>, is not a rate limiting factor in accordance with the experimental zero-order of the reaction in **1a**. As expected, the energy barrier for the oxidative addition with (*E*)- $\beta$ -iodostyrene (**1aa**) is significantly lower (18.6 kcal mol<sup>-1</sup>) (Figure 5). The fact that the oxidative addition is not rate limiting suggests that all RX compounds react equally fast (assuming equal insolubility of KI and KBr affecting the V<sub>(X,3a)</sub> to V<sub>(OPiv,3a)</sub> equilibrium in DCE) as the energetic span determined by the resting state V<sub>(OPiv,3a)</sub> and the C(sp<sup>3</sup>)-H bond activation step is independent of the halide ion (Supporting Information Figure S5A). In accordance with this, the reaction performed with (*E*)- $\beta$ -iodostyrene (**1aa**) gave a similar result as with (*E*)- $\beta$ -bromostyrene (**1a**) (Table 1, entries 2 and 5).

The oxidative addition energy barrier was also calculated for other bromoalkenes (Figure 5). (2,2-Dibromoethenyl)benzene (**8a**)<sup>9</sup> features a lower barrier than **1a** in accordance with the additional geminal bromine atom. With (*E*)-(2-bromovinyl)-cyclohexane (**1c**) the energy increases versus **1a** based on the removal of the activating phenyl. Finally, bromobenzene (**4a**) shows the lowest energy value (16.2 kcal mol<sup>-1</sup>) which is also still lower than the C(sp<sup>3</sup>)-H bond activation barrier, indicating that the oxidative addition is not a limiting factor.

**Stability of the Resting State V<sub>(OPiv,3)</sub> Featuring Different 3-Alkenyl-*N*-picolinoylcyclohexanamine Products (**3**).** Besides anion X, the electrophile has an influence on the stability of the catalyst's resting state. Therefore, the effect of the double bond in the C3-substituent of the coordinated reaction product **3** in V<sub>(Br,3)</sub> has been investigated in more detail. Replacing the ethylene Ph substituent in V<sub>(Br,3a)</sub> by Cy V<sub>(Br,3c)</sub> decreases the energy of the resting state by 3.9 kcal mol<sup>-1</sup>, while changing Ph by <sup>t</sup>Bu does not have an impact on the energy of the resting state V<sub>(Br,3b)</sub> (Scheme 7). With ethenyl conjugated to phenyl (V<sub>(Br,3a)</sub>), the electron density at the double bond is lower than that with the alkyl substituent Cy (V<sub>(Br,3c)</sub>). This difference results in a weaker  $\eta^2$  interaction between Pd(II) and the double bond. Consequently, the resting state V<sub>(Br,3c)</sub> is stabilized compared to V<sub>(Br,3a)</sub> and the energetic span versus TSI<sub>OPiv</sub> increases. A <sup>t</sup>Bu is also an electron donating group but its sterics significantly weakens the  $\eta^2$  interaction in V<sub>(Br,3b)</sub>. This counterbalancing effect brings it to the same energy level of a Ph substituent (V<sub>(Br,3b)</sub> versus V<sub>(Br,3a)</sub> is 0.9 kcal mol<sup>-1</sup>). Consistently, the trend in stability of V<sub>(Br,3)</sub> with Cy, Ph and <sup>t</sup>Bu substituents correlates well with the  $\pi$ -donation and back-donation interactions between the ethenyl C=C bond and the Pd d<sub>x<sup>2</sup>-y<sup>2</sup></sub> orbital (Supporting Information Table S11). These DFT results are in accordance with the experimental results, where for **3c** (R = Cy), the starting material **2a** was recovered in 62%, while for **3a** (R = Ph) and **3b** (R = <sup>t</sup>Bu), high yields and high conversions of substrate **2a** were observed in 24 h (Scheme 7). When 50 mol % of reaction product **3a** was added to the model reaction of **1a** and **2a**, the conversion to and yield of **3a** in 3 h dropped significantly (Scheme 5B). A higher concentration of **3a** inhibits catalysis by hampering the decomplexation of **3a** from V<sub>(Br,3a)</sub> via V<sub>(OPiv,3a)</sub>. This is required to allow subsequent complexation of substrate **2a**, hereby providing starting complex I<sub>OPiv</sub> for another catalytic cycle in accordance to the computed mechanism (Scheme 6). A similar observation was made when adding 50 mol % of **3d** to the reaction of **1d** and **2a** (Scheme 5B). These inhibitions rationalize the experimental order of 0.25 for the reaction in Pd(OAc)<sub>2</sub>.

**Catalyst Resting State for C(sp<sup>3</sup>)-H Arylation versus Alkenylation.** With 3-phenylated product **5a**, the weaker coordination of the aromatic ring compared with the  $\eta^2$  double bond in 3-alkenylated products **3** lifts the energy of V<sub>(Br,5a)</sub> versus V<sub>(Br,3a)</sub> by 16.3 kcal mol<sup>-1</sup> (Figure 5). This result implies that V<sub>(Br,5a)</sub> is not the resting state in the arylation reaction but rather I', with a slightly decreased energetic span with rate limiting TSI<sub>OPiv</sub> (33.9 for **5a** versus 35.2 for **3a**) kcal mol<sup>-1</sup> (Figure 5). As observed for **3a**, the bromide complex V<sub>(Br,5a)</sub> is more stable (2.3 kcal mol<sup>-1</sup>) than the pivalate V<sub>(OPiv,5a)</sub>. The similar overall energy span for arylation justifies why the reaction conditions developed for alkenylation could be applied to arylation without further modification (Scheme 3). However, alkenylation is a much more difficult reaction. A higher conversion of substrate **2a** means a higher concen-

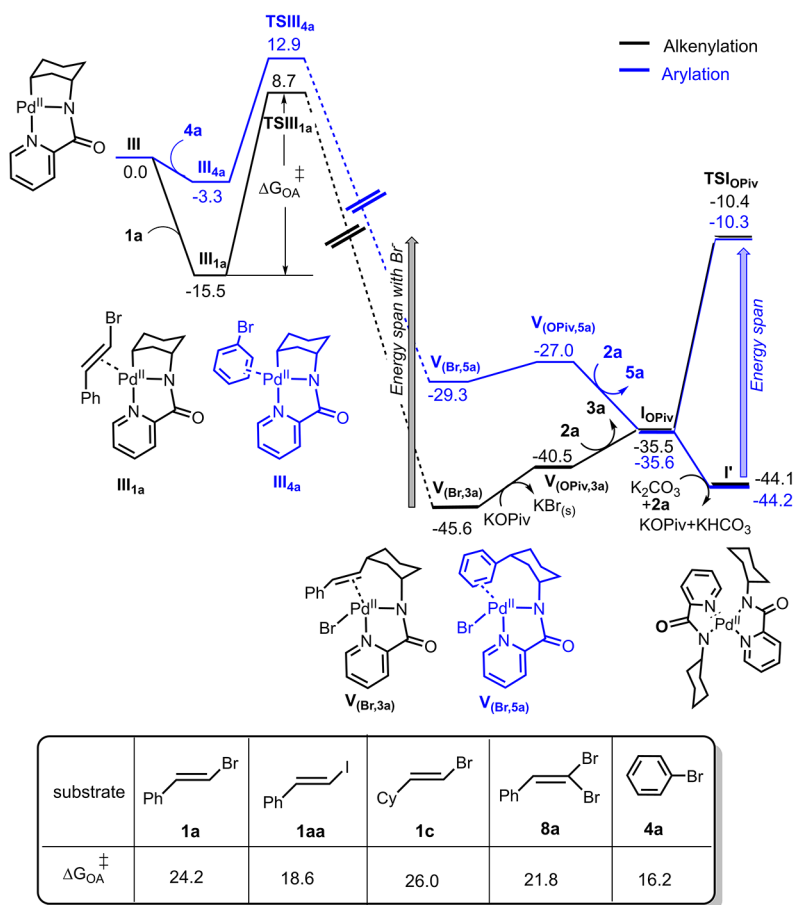
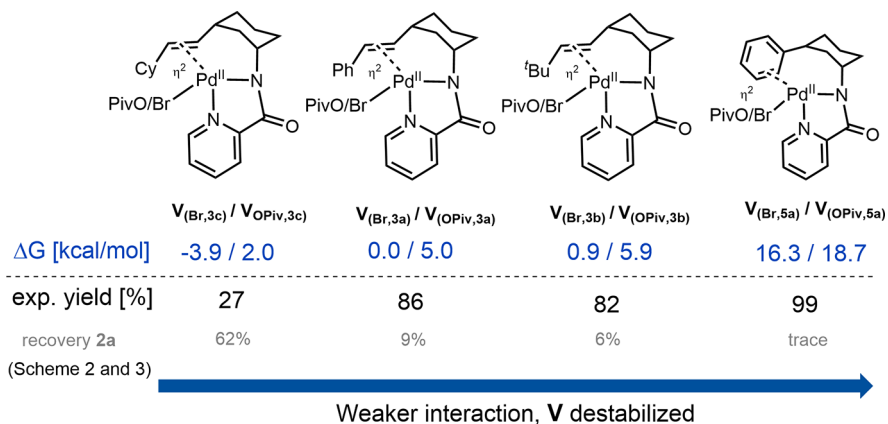


**Figure 5.** Energy diagram for the alkenylation reaction with reactant **1a** (black) and the arylation reaction with reactant **4a** (blue). Barriers for the oxidative addition step,  $\Delta G_{\text{OA}}^{\ddagger}$ , for different electrophiles and halide leaving groups are also shown. Gibbs free energies in  $\text{kcal mol}^{-1}$ .

**Scheme 7.** Effect of C3-Substituent in Product 3/5 on the Stability of  $V_{(\text{Br},3/5)}$  and  $V_{(\text{OPiv},3/5)}$  (Gibbs Free Energies in  $\text{kcal mol}^{-1}$ )



tration of reaction product **3a**, making its release of the resting state  $V_{(\text{Br},3a)}$  progressively more difficult. On the contrary, in arylation a higher conversion of substrate **2a** means a lower concentration of **2a**, promoting  $I_{\text{OPiv}}$  versus resting state  $I'$ , hereby making the reaction easier.

## CONCLUSIONS

In summary, we have developed an efficient Pd-catalyzed reaction for the  $\gamma\text{-C}(\text{sp}^3)\text{-H}$  alkenylation of cyclohexanamines, employing a picolinoylamine bidentate directing group with

readily available alkenyl bromide coupling partners under silver-free conditions. Even very challenging heterocyclic substrates (piperidinamine and tetrahydro-2H-pyranamine) were compatible. The method exhibits a broad alkenyl reactant scope with excellent functional group tolerance and regio- and stereospecificity. The underlying reaction mechanism has been studied experimentally by using kinetics and a KIE, and theoretically by density functional theory. The calculations show that the reaction follows a Pd(II)/Pd(IV) pathway in which the transition state of the  $\text{C}(\text{sp}^3)\text{-H}$  activation occurs

through a CMD mechanism. Interestingly, the oxidative addition to form a Pd(IV) species is not rate-determining. The overall energy barrier is determined by the C(sp<sup>3</sup>)–H activation and the reaction product formed in the catalytic cycle, which strongly coordinates to the palladium center. Addition of a catalytic amount of KO<sup>t</sup>Piv is beneficial for the conversion of substrate, resulting in substantially higher product yield. The additive is involved in the C–H activation mechanism, i.e., CMD, as well as in the anion exchange in the catalyst resting state V<sub>(Br,3)</sub> providing a more reactive pivalate complex V<sub>(OPiv,3)</sub>. This endergonic step only proceeds efficiently by precipitation of KBr and hence the importance of the reaction solvent. Precipitation makes the use of superstoichiometric metal reagents redundant. Insights into the electronic structure of V<sub>(Br,3)</sub> revealed that alkenyl groups featuring electron-withdrawing substituents leads to a weaker η<sup>2</sup> interaction between π of alkene of the reaction product 3 and the Pd(II). Consequently, the resting state V<sub>(Br,3)</sub> is destabilized and the overall barrier decreases allowing easier decomplexation of the reaction product 3 via V<sub>(OPiv,3)</sub>. Electron donating substituents therefore provide poorer conversion. This trend matches the experimental performance of the different alkene substituents. I', formed by coordination of a second substrate molecule to I<sub>OPiv</sub> and deprotonation, is higher in energy than V<sub>(Br,3)</sub>. However, it can become the resting state of the catalytic cycle with weaker Pd(II) coordinating electrophiles, such as the arene of product 5. The slightly lower overall energy span (TSI<sub>OPiv</sub> - I' versus TSI<sub>OPiv</sub> - V<sub>(Br,3)</sub>) rationalizes why our developed method is also effective for the γ-C(sp<sup>3</sup>)–H arylation involving (hetero)aryl bromides. Here V<sub>(Br,5)</sub> does not act as a resting state and both V<sub>(Br,5)</sub> and V<sub>(OPiv,5)</sub> are substantially higher in energy based on a weaker coordination of the arene of product 5 to Pd(II), resulting in another catalyst resting state (I'). Nevertheless, γ-C(sp<sup>3</sup>)–H arylation is a much easier reaction than γ-C(sp<sup>3</sup>)–H alkenylation when considering concentrations. After all, a higher conversion of substrate 2 favors I<sub>OPiv</sub> versus I', while at this higher conversion, there is more reaction product 3/5 present, favoring V<sub>(Br,3/5)</sub> versus I<sub>OPiv</sub>. The difference in the resting state, i.e., I' for arylation versus V<sub>(Br,3)</sub> for alkenylation, therefore directly determines performance as the former complex is not affected by product coordination while the latter is.

## ■ ASSOCIATED CONTENT

### SI Supporting Information

The Supporting Information is available free of charge at <https://pubs.acs.org/doi/10.1021/acscatal.3c04152>.

Detailed optimization data, experimental procedures, characterization data, and copies of NMR spectra of all compounds, DFT computations, and crystallographic data (PDF)

### Accession Codes

CCDC 2232137 (for 3c), 2232138 (for 3f), 2232139 (for 5a), 2232140 (for 7d) contain the supplementary crystallographic data for this paper. These data are provided free of charge by contacting the Cambridge Crystallographic Data Centre.

## ■ AUTHOR INFORMATION

### Corresponding Authors

Ainara Nova – Department of Chemistry, Hylleraas Centre for Quantum Molecular Sciences and Centre for Materials

Science and Nanotechnology, University of Oslo, N-0315

Oslo, Norway; Email: [a.n.flores@kjemi.uio.no](mailto:a.n.flores@kjemi.uio.no)

Bert U. W. Maes – Division of Organic Synthesis, Department of Chemistry, University of Antwerp, B-2020 Antwerp, Belgium; [orcid.org/0000-0003-0431-7606](https://orcid.org/0000-0003-0431-7606); Email: [bert.maes@uantwerpen.be](mailto:bert.maes@uantwerpen.be)

## Authors

Karthik Gadde – Division of Organic Synthesis, Department of Chemistry, University of Antwerp, B-2020 Antwerp, Belgium; [orcid.org/0000-0001-6624-4129](https://orcid.org/0000-0001-6624-4129)

Narendraprasad Reddy Bheemireddy – Division of Organic Synthesis, Department of Chemistry, University of Antwerp, B-2020 Antwerp, Belgium

Juliane Heitkämper – Department of Chemistry, Hylleraas Centre for Quantum Molecular Sciences and Centre for Materials Science and Nanotechnology, University of Oslo, N-0315 Oslo, Norway; Institute for Theoretical Chemistry, University of Stuttgart, D-70569 Stuttgart, Germany

Complete contact information is available at:

<https://pubs.acs.org/10.1021/acscatal.3c04152>

## Author Contributions

<sup>†</sup>K.G., N.R.B., and J.H. contributed equally to this work.

## Notes

The authors declare no competing financial interest.

## ■ ACKNOWLEDGMENTS

This work is dedicated to Professor Masahiro Miura for his outstanding contribution to catalytic organic synthesis. The research was funded by FWO-Flanders (Senior Research Project grant no. GOA2820N) and the Hercules Foundation. J.H. acknowledges the financial support received in the form of a Ph.D. scholarship from the Studienstiftung des Deutschen Volkes (German National Academic Foundation). J.H. and A.N. thank the Norwegian Metacenter for Computational Science (NOTUR) for computational resources (project number nn4654k). A.N. acknowledges the support from the Research Council of Norway through the Centre of Excellence (no. 262695) and for its FRINATEK program (no. 314321). All authors thank Prof. Christophe Vande Velde for X-ray analysis, Dr. H. Y. Vincent Ching and Glenn Van Haesendonck for analytical support, Philippe Franck for technical support, and Mathias Bal for assistance with the VTNA.

## ■ REFERENCES

- (1) For selected reviews, see: (a) Sambiagio, C.; Schönbauer, D.; Blicke, R.; Dao-Huy, T.; Pototschnig, G.; Schaaf, P.; Wiesinger, T.; Zia, M. F.; Wencel-Delord, J.; Besset, T.; Maes, B. U. W.; Schnürch, M. A Comprehensive Overview of Directing Groups Applied in Metal-Catalysed C–H Functionalisation Chemistry. *Chem. Soc. Rev.* **2018**, *47*, 6603–6743. (b) Rej, S.; Ano, Y.; Chatani, N. Bidentate Directing Groups: An Efficient Tool in C–H Bond Functionalization Chemistry for the Expedient Construction of C–C Bonds. *Chem. Rev.* **2020**, *120*, 1788–1887. (c) Liu, B.; Romine, A. M.; Rubel, C. Z.; Engle, K. M.; Shi, B.-F. Transition-Metal-Catalyzed, Coordination-Assisted Functionalization of Nonactivated C(sp<sup>3</sup>)–H Bonds. *Chem. Rev.* **2021**, *121*, 14957–15074. (d) Jacob, C.; Maes, B. U. W.; Evano, G. Transient Directing Groups in Metal–Organic Cooperative Catalysis. *Chem.—Eur. J.* **2021**, *27*, 13899–13952. (e) Sen, S.; Das, J.; Maiti, D. Strategies to Transform Remote C(sp<sup>3</sup>)–H Bonds of Amino Acid Derivatives. *Tetrahedron Chem.* **2022**, *1*, No. 100005. (f) Ali, W.; Prakash, G.; Maiti, D. Recent Development in Transition Metal-Catalysed C–H Olefination. *Chem. Sci.* **2021**, *12*, 2735–2759.

- (g) Bhattacharya, T.; Dutta, S.; Maiti, D. Deciphering the Role of Silver in Palladium-Catalyzed C–H Functionalizations. *ACS Catal.* **2021**, *11*, 9702–9714. (h) Mondal, A.; van Gemmeren, M. Silver-Free C–H Activation: Strategic Approaches towards Realizing the Full Potential of C–H Activation in Sustainable Organic Synthesis. *Angew. Chem., Int. Ed.* **2022**, *61*, No. e202210825.
- (2) Remote-C(sp<sup>3</sup>)-H alkenylation of alkanamines with alkenyl iodides: (a) He, G.; Chen, G. A Practical Strategy for the Structural Diversification of Aliphatic Scaffolds through the Palladium-Catalyzed Picolinamide-Directed Remote Functionalization of Unactivated C(sp<sup>3</sup>)-H Bonds. *Angew. Chem., Int. Ed.* **2011**, *50*, 5192–5196. (b) Seki, A.; Takahashi, Y. Pd-Catalyzed Methylene  $\gamma$ -C(sp<sup>3</sup>)-H Alkenylation of *N*-picolinoylcycloalkylamines with Alkenyl Iodides Promoted by 2-*tert*-Butyl-1,4-benzoquinone. *Tetrahedron Lett.* **2021**, *74*, No. 153130.
- (3) Remote-C(sp<sup>3</sup>)-H alkenylation of carbonyl compounds (carboxylic acids and ketones) with alkenyl iodides: (a) Gutekunst, W. R.; Gianatassio, R.; Baran, P. S. Sequential Csp<sup>3</sup>-H Arylation and Olefination: Total Synthesis of the Proposed Structure of Pipericyclobutanamide A. *Angew. Chem., Int. Ed.* **2012**, *51*, 7507–7510. (b) Gutekunst, W. R.; Baran, P. S. Applications of C–H Functionalization Logic to Cyclobutane Synthesis. *J. Org. Chem.* **2014**, *79*, 2430–2452. (c) Wang, B.; Lu, C.; Zhang, S.-Y.; He, G.; Nack, W. A.; Chen, G. Palladium-Catalyzed Stereoretentive Olefination of Unactivated C(sp<sup>3</sup>)-H Bonds with Vinyl Iodides at Room Temperature: Synthesis of  $\beta$ -Vinyl  $\alpha$ -Amino Acids. *Org. Lett.* **2014**, *16*, 6260–6263. (d) Shan, G.; Huang, G.; Rao, Y. Palladium-Catalyzed Unactivated  $\beta$ -Methylene C(sp<sup>3</sup>)-H Bond Alkenylation of Aliphatic Amides and its Application in a Sequential C(sp<sup>3</sup>)-H/C(sp<sup>2</sup>)-H Bond Alkenylation. *Org. Biomol. Chem.* **2015**, *13*, 697–701. (e) Zhang, Y.-F.; Zhao, H.-W.; Wang, H.; Wei, J.-B.; Shi, Z.-J. Readily Removable Directing Group Assisted Chemo- and Regioselective C(sp<sup>3</sup>)-H Activation by Palladium Catalysis. *Angew. Chem., Int. Ed.* **2015**, *54*, 13686–13690. (f) Chapman, L. M.; Beck, J. C.; Wu, L.; Reisman, S. E. Enantioselective Total Synthesis of (+)-Psiguadial B. *J. Am. Chem. Soc.* **2016**, *138*, 9803–9806. (g) Thrimurtulu, N.; Khan, S.; Maity, S.; Volla, C. M. R.; Maiti, D. Palladium Catalyzed Direct Aliphatic  $\gamma$ C(sp<sup>3</sup>)-H Alkenylation with Alkenes and Alkenyl Iodides. *Chem. Commun.* **2017**, *53*, 12457–12460. (h) Wu, Q.-F.; Shen, P.-X.; He, J.; Wang, X.-B.; Zhang, F.; Shao, Q.; Zhu, R.-Y.; Mapelli, C.; Qiao, J. X.; Poss, M. A.; Yu, J.-Q. Formation of  $\alpha$ -Chiral Centers by Asymmetric  $\beta$ -C(sp<sup>3</sup>)-H Arylation, Alkenylation, and Alkynylation. *Science* **2017**, *355*, 499–503. (i) Zhu, R.-Y.; Li, Z.-Q.; Park, H. S.; Senanayake, C. H.; Yu, J.-Q. Ligand-Enabled  $\gamma$ -C(sp<sup>3</sup>)-H Activation of Ketones. *J. Am. Chem. Soc.* **2018**, *140*, 3564–3568. (j) Wu, Q.-F.; Wang, X.-B.; Shen, P.-X.; Yu, J.-Q. Enantioselective C–H Arylation and Vinylation of Cyclobutyl Carboxylic Amides. *ACS Catal.* **2018**, *8*, 2577–2581. (k) Minami, T.; Fukuda, K.; Hoshiya, N.; Fukuda, H.; Watanabe, M.; Shuto, S. Synthesis of Enantiomerically Pure 1,2,3-Trisubstituted Cyclopropane Nucleosides Using Pd-Catalyzed Substitution via Directing Group-Mediated C(sp<sup>3</sup>)-H Activation as a Key Step. *Org. Lett.* **2019**, *21*, 656–659. (l) Liu, Y.; Wang, Y.; Dai, W.; Huang, W.; Li, Y.; Liu, H. Palladium-Catalyzed C(sp<sup>3</sup>)-H Glycosylation for the Synthesis of C-Alkyl Glycoamino Acids. *Angew. Chem., Int. Ed.* **2020**, *59*, 3491–3494.
- (4) Activated alkenes have been used in oxidative alkenylation: (a) Park, H.; Li, Y.; Yu, J.-Q. Utilizing Carbonyl Coordination of Native Amides for Palladium-Catalyzed C(sp<sup>3</sup>)-H Olefination. *Angew. Chem., Int. Ed.* **2019**, *58*, 11424–11428. (b) Zhuang, Z.; Yu, J.-Q. Pd(II)-Catalyzed Enantioselective  $\gamma$ -C(sp<sup>3</sup>)-H Functionalizations of Free Cyclopropylmethylamines. *J. Am. Chem. Soc.* **2020**, *142*, 12015–12019. (c) Bhattacharya, T.; Baroliya, P. K.; Al-Thabaiti, S. A.; Maiti, D. Simplifying the Synthesis of Nonproteinogenic Amino Acids via Palladium-Catalyzed  $\delta$ -Methyl C–H Olefination of Aliphatic Amines and Amino Acids. *JACS Au* **2023**, *3*, 1975–1983. (d) Das, J.; Pal, T.; Ali, W.; Sahoo, S. R.; Maiti, D. Pd-Catalyzed Dual- $\gamma$ -1,1-C(sp<sup>3</sup>)-H Activation of Free Aliphatic Acids with Allyl-O Moieties. *ACS Catal.* **2022**, *12*, 11169–11176. (e) see reference 3g.
- (5) Ricci, A.; Bernardi, L. *Methodologies in Amine Synthesis: Challenges and Applications*. Wiley: Weinheim, 2021.
- (6) For selected reviews, see: (a) He, C.; Whitehurst, W. G.; Gaunt, M. J. Palladium-Catalyzed C(sp<sup>3</sup>)-H Bond Functionalization of Aliphatic Amines. *Chem.* **2019**, *5*, 1031–1058. (b) Trowbridge, A.; Walton, S. M.; Gaunt, M. J. New Strategies for the Transition-Metal Catalyzed Synthesis of Aliphatic Amines. *Chem. Rev.* **2020**, *120*, 2613–2692.
- (7) Zaitsev, V. G.; Shabashov, D.; Daugulis, O. Highly Regioselective Arylation of sp<sup>3</sup> C–H Bonds Catalyzed by Palladium Acetate. *J. Am. Chem. Soc.* **2005**, *127*, 13154–13155.
- (8) Hartwig, J. F.; Larsen, M. A. Undirected, Homogeneous C–H Bond Functionalization: Challenges and Opportunities. *ACS Cent. Sci.* **2016**, *2*, 281–292.
- (9) Biswas, S.; Van Steijvoort, B. F.; Waeterschoot, M.; Bheemireddy, N. R.; Evano, G.; Maes, B. U. W. Expedient Synthesis of Bridged Bicyclic Nitrogen Scaffolds via Orthogonal Tandem Catalysis. *Angew. Chem., Int. Ed.* **2021**, *60*, 21988–21996.
- (10) (a) Giri, R.; Lan, Y.; Liu, P.; Houk, K. N.; Yu, J.-Q. Understanding Reactivity and Stereoselectivity in Palladium-Catalyzed Diastereoselective sp<sup>3</sup> C–H Bond Activation: Intermediate Characterization and Computational Studies. *J. Am. Chem. Soc.* **2012**, *134*, 14118–14126. (b) Yang, Y.-F.; Hong, X.; Yu, J.-Q.; Houk, K. N. Experimental–Computational Synergy for Selective Pd(II)-Catalyzed C–H Activation of Aryl and Alkyl Groups. *Acc. Chem. Res.* **2017**, *50*, 2853–2860. (c) Rodrigalvarez, J.; Reeve, L. A.; Miró, J.; Gaunt, M. J. Pd(II)-Catalyzed Enantioselective C(sp<sup>3</sup>)-H Arylation of Cyclopropanes and Cyclobutanes Guided by Tertiary Alkylamines. *J. Am. Chem. Soc.* **2022**, *144*, 3939–3948. (d) Hao, W.; Bay, K. L.; Harris, C. F.; King, D. S.; Guzei, I. A.; Aristov, M. M.; Zhuang, Z.; Plata, R. E.; Hill, D. E.; Houk, K. N.; Berry, J. F.; Yu, J.-Q.; Blackmond, D. G. Probing Catalyst Speciation in Pd-MPAAM-Catalyzed Enantioselective C(sp<sup>3</sup>)-H Arylation: Catalyst Improvement via Destabilization of Off-Cycle Species. *ACS Catal.* **2021**, *11*, 11040–11048. (e) Melot, R.; Zuccarello, M.; Cavalli, D.; Niggli, N.; Devereux, M.; Bürgi, T.; Baudoin, O. Palladium(0)-Catalyzed Enantioselective Intramolecular Arylation of Enantiotopic Secondary C–H Bonds. *Angew. Chem., Int. Ed.* **2021**, *60*, 7245–7250. (f) Zhang, H.; Wang, H.-Y.; Luo, Y.; Chen, C.; Cao, Y.; Chen, P.; Guo, Y.-L.; Lan, Y.; Liu, G. Regioselective Palladium-Catalyzed C–H Bond Trifluoroethylation of Indoles: Exploration and Mechanistic Insight. *ACS Catal.* **2018**, *8*, 2173–2180. (g) Romero, E. A.; Chen, G.; Gembicky, M.; Jazzar, R.; Yu, J.-Q.; Bertrand, G. Understanding the Activity and Enantioselectivity of Acetyl-Protected Aminoethyl Quinoline Ligands in Palladium-Catalyzed  $\beta$ -C(sp<sup>3</sup>)-H Bond Arylation Reactions. *J. Am. Chem. Soc.* **2019**, *141*, 16726–16733. (h) Ghouilem, J.; Tran, C.; Grimblat, N.; Retailleau, P.; Alami, M.; Gandon, V.; Messaoudi, S. Diastereoselective Pd-Catalyzed Anomeric C(sp<sup>3</sup>)-H Activation: Synthesis of  $\alpha$ -(Hetero)aryl C-Glycosides. *ACS Catal.* **2021**, *11*, 1818–1826.
- (11) Smalley, A. P.; Gaunt, M. J. Mechanistic Insights into the Palladium-Catalyzed Aziridination of Aliphatic Amines by C–H Activation. *J. Am. Chem. Soc.* **2015**, *137*, 10632–10641.
- (12) Rodrigalvarez, J.; Nappi, M.; Azuma, H.; Flodén, N. J.; Burns, M. E.; Gaunt, M. J. Catalytic C(sp<sup>3</sup>)-H Bond Activation in Tertiary Alkylamines. *Nat. Chem.* **2020**, *12*, 76–81.
- (13) Lian, B.; Zhang, L.; Chass, G. A.; Fang, D.-C. Pd(OAc)<sub>2</sub>-Catalyzed C–H Activation/C–O Cyclization: Mechanism, Role of Oxidant-Probed by Density Functional Theory. *J. Org. Chem.* **2013**, *78*, 8376–8385.
- (14) (a) Provencher, P. A.; Hoskin, J. F.; Wong, J. J.; Chen, X.; Yu, J.-Q.; Houk, K. N.; Sorensen, E. J. Pd(II)-Catalyzed Synthesis of Benzocyclobutenes by  $\beta$ -Methylene-Selective C(sp<sup>3</sup>)-H Arylation of a Transient Directing Group. *J. Am. Chem. Soc.* **2021**, *143*, 20035–20041. (b) Ha, H.; Choi, H. J.; Park, H.; Gwon, Y.; Lee, J.; Kwak, J.; Kim, M.; Jung, B. Pd-Catalyzed Regio- and Stereoselective sp<sup>3</sup> C–H Arylation of Primary Aliphatic Amines: Mechanistic Studies and Synthetic Applications. *Eur. J. Org. Chem.* **2021**, *2021*, 1136–1145. (c) Martínez-Mingo, M.; García-Viada, A.; Alonso, I.; Rodríguez, N.; Gómez Arrayás, R.; Carretero, J. C. Overcoming the

Necessity of  $\gamma$ -Substitution in  $\delta$ -C(sp<sup>3</sup>)-H Arylation: Pd-Catalyzed Derivatization of  $\alpha$ -Amino Acids. *ACS Catal.* **2021**, *11*, 5310–5317. (d) Yang, Y.-F.; Chen, G.; Hong, X.; Yu, J.-Q.; Houk, K. N. The Origins of Dramatic Differences in Five-Membered vs Six-Membered Chelation of Pd(II) on Efficiency of C(sp<sup>3</sup>)-H Bond Activation. *J. Am. Chem. Soc.* **2017**, *139*, 8514–8521. (e) Antermite, D.; White, A. J. P.; Casarrubios, L.; Bull, J. A. On the Mechanism and Selectivity of Palladium-Catalyzed C(sp<sup>3</sup>)-H Arylation of Pyrrolidines and Piperidines at Unactivated C4 Positions: Discovery of an Improved Dimethylaminoquinoline Amide Directing Group. *ACS Catal.* **2023**, *13*, 9597–9615.

(15) Bonney, K. J.; Schoenebeck, F. Experiment and Computation: A Combined Approach to Study the Reactivity of Palladium Complexes in Oxidation States 0 to IV. *Chem. Soc. Rev.* **2014**, *43*, 6609–6638.

(16) For reviews and book chapters on C(sp<sup>3</sup>)-H functionalization in saturated heterocycles, see: (a) Mitchell, E. A.; Peschiulli, A.; Lefevre, N.; Meerpoel, L.; Maes, B. U. W. Direct  $\alpha$ -Functionalization of Saturated Cyclic Amines. *Chem.—Eur. J.* **2012**, *18*, 10092–10142. (b) Liu, G.-Q.; Opatz, T., Recent Advances in the Synthesis of Piperidines: Functionalization of Preexisting Ring Systems. In *Advances in Heterocyclic Chemistry*, Scriven, E. F. V.; Ramsden, C. A., Eds.: 2018; Vol. 125, pp 107–234 DOI: 10.1016/bs.aihch.2017.10.001. (c) Antermite, D.; Bull, J. A. Transition Metal-Catalyzed Directed C(sp<sup>3</sup>)-H Functionalization of Saturated Heterocycles. *Synthesis* **2019**, *51*, 3171–3204. (d) Dutta, S.; Li, B.; Rickertsen, D. R. L.; Valles, D. A.; Seidel, D. C-H Bond Functionalization of Amines: A Graphical Overview of Diverse Methods. *SynOpen* **2021**, *05*, 173–228. (e) Piticari, A.-S.; Larionova, N.; Bull, J. A., C-H Functionalization of Saturated Heterocycles Beyond the C2 Position. In *Transition-Metal-Catalyzed C-H Functionalization of Heterocycles*, Punniyamurthy, T.; Kumar, A., Eds.: Wiley, 2023; pp 567–607 DOI: 10.1002/9781119774167.ch13.

(17) (a) Biswas, S.; Bheemireddy, N. R.; Bal, M.; Van Steijvoort, B. F.; Maes, B. U. W. Directed C-H Functionalization Reactions with a Picolinamide Directing Group: Ni-Catalyzed Cleavage and Byproduct Recycling. *J. Org. Chem.* **2019**, *84*, 13112–13123. (b) Van Steijvoort, B. F.; Kaval, N.; Kulago, A. A.; Maes, B. U. W. Remote Functionalization: Palladium-Catalyzed C5(sp<sup>3</sup>)-H Arylation of 1-Boc-3-aminopiperidine through the Use of a Bidentate Directing Group. *ACS Catal.* **2016**, *6*, 4486–4490.

(18) For a review, see: Gao, P.; Rahman, M. M.; Zamalloa, A.; Feliciano, J.; Szostak, M. Classes of Amides that Undergo Selective N-C Amide Bond Activation: The Emergence of Ground-State Destabilization. *J. Org. Chem.* **2023**, *88*, 13371–13391.

(19) (a) Burés, J. A Simple Graphical Method to Determine the Order in Catalyst. *Angew. Chem., Int. Ed.* **2016**, *55*, 2028–2031. (b) Burés, J. Variable Time Normalization Analysis: General Graphical Elucidation of Reaction Orders from Concentration Profiles. *Angew. Chem., Int. Ed.* **2016**, *55*, 16084–16087. (c) Nielsen, C. D. T.; Burés, J. Visual kinetic analysis. *Chem. Sci.* **2019**, *10*, 348–353.

(20) Zhao, Y.; Truhlar, D. G. The M06 Suite of Density Functionals for Main Group Thermochemistry, Thermochemical Kinetics, Noncovalent Interactions, Excited States, and Transition Elements: Two New Functionals and Systematic Testing of Four M06-Class Functionals and 12 other Functionals. *Theor. Chem. Acc.* **2008**, *120*, 215–241.

(21) (a) Alharis, R. A.; McMullin, C. L.; Davies, D. L.; Singh, K.; Macgregor, S. A. The Importance of Kinetic and Thermodynamic Control when Assessing Mechanisms of Carboxylate-Assisted C-H Activation. *J. Am. Chem. Soc.* **2019**, *141*, 8896–8906. (b) Altus, K. M.; Love, J. A. The Continuum of Carbon-Hydrogen (C-H) Activation Mechanisms and Terminology. *Commun. Chem.* **2021**, *4*, 173. (c) Balcells, D.; Clot, E.; Eisenstein, O. C-H Bond Activation in Transition Metal Species from a Computational Perspective. *Chem. Rev.* **2010**, *110*, 749–823. (d) Davies, D. L.; Macgregor, S. A.; McMullin, C. L. Computational Studies of Carboxylate-Assisted C-H Activation and Functionalization at Group 8–10 Transition Metal

Centers. *Chem. Rev.* **2017**, *117*, 8649–8709. (e) Ghosh, S.; Shilpa, S.; Athira, C.; Sunoj, R. B. Role of Additives in Transition Metal Catalyzed C-H Bond Activation Reactions: A Computational Perspective. *Top. Catal.* **2022**, *65*, 141–164. (f) Boutadla, Y.; Davies, D. L.; Macgregor, S. A.; Poblador-Bahamonde, A. I. Mechanisms of C-H Bond Activation: Rich Synergy between Computation and Experiment. *Dalton Trans.* **2009**, 5820–5831.

(22) Topczewski, J. J.; Sanford, M. S. Carbon-Hydrogen (C-H) Bond Activation at Pd<sup>IV</sup>: A Frontier in C-H Functionalization Catalysis. *Chem. Sci.* **2015**, *6*, 70–76.

(23) Reed, A. E.; Curtiss, L. A.; Weinhold, F. Intermolecular Interactions from a Natural Bond Orbital, Donor-Acceptor Viewpoint. *Chem. Rev.* **1988**, *88*, 899–926.

(24) Zaitsev, V. G.; Daugulis, O. Catalytic Coupling of Haloolefins with Anilides. *J. Am. Chem. Soc.* **2005**, *127*, 4156–4157.

(25) Kozuch, S.; Shaik, S. How to Conceptualize Catalytic Cycles? The Energetic Span Model. *Acc. Chem. Res.* **2011**, *44*, 101–110.

(26) García-Cuadrado, D.; de Mendoza, P.; Braga, A. A. C.; Maseras, F.; Echavarren, A. M. Proton-Abstraction Mechanism in the Palladium-Catalyzed Intramolecular Arylation: Substituent Effects. *J. Am. Chem. Soc.* **2007**, *129*, 6880–6886.